

A STUDY OF THE CHIRP Z-TRANSFORM
AND ITS APPLICATIONS

by

STEVE ALAN SHILLING

B. S., Kansas State University, 1970

9984

A MASTER'S REPORT

submitted in partial fulfillment of the

requirements for the degree

MASTER OF SCIENCE

Department of Electrical Engineering

KANSAS STATE UNIVERSITY
Manhattan, Kansas

1972

Approved by:

Nasir Ahmed
Major Professor

D
2668
R 4
1972
S 43
copy 2

TABLE OF CONTENTS

<u>Chapter</u>		<u>Page</u>
I INTRODUCTION		1
II THE CHIRP Z-TRANSFORM		
The Z-Transform		2
Evaluating the Z-Transform of a Finite Sequence		6
A Special Case of the CZT		10
Computation of the CZT		11
III APPLICATION CONSIDERATIONS		
Enhancement of Poles		20
High Resolution, Narrow Band Spectra		24
Limitations		37
IV SUMMARY AND RECOMMENDATIONS		
Summary and Conclusions		39
Recommendations for further Investigation .		40
SELECTED REFERENCES		41
APPENDIX		42
ACKNOWLEDGEMENT		50

LIST OF FIGURES

<u>Figure</u>	<u>Title</u>	<u>Page</u>
2-1	The ideal sampling operation	3
2-2	S-plane representations and Fourier transforms of $x(t)$ and $x^*(t)$	5
2-3	Examples of two contours in both the 'S' and 'Z' planes	7
2-4	A general CZT contour with $M=8$	9
2-5	Contour for an 8-point FFT	12
2-6	Standard FFT signal flow graph, $N=8$	13
2-7	An illustration of the steps in the CZT algorithm	16
2-8	Block diagram of the way the FFT is used in computing the convolution in the CZT	17
3-1	Four contours used to show the effect of moving the CZT contour closer to the pole .	21
3-2	Example of pole enhancement using four different CZT contours	22
3-3	FFT and CZT contours for a three pole system .	25
3-4	$ H(j\omega) ^2$ as computed by the FFT (78 Hz. resolution)	26
3-5	$ H(s) ^2$ as computed by the CZT (78 Hz. resolution)	27
3-6	$ H(s) ^2$ as computed by the CZT (39 Hz. resolution)	28
3-7	Frequency shifted FFTs ($N=8$)	30
3-8	Examples of FFT and CZT contours	31
3-9	A truncated filter impulse response, a plot of Eq. (3-3)	34

CHAPTER I

INTRODUCTION

The z-transform is of significant importance in processing discrete data. With the development of the Fast Fourier transform (FFT), it became economically practical to numerically evaluate the z-transform of a finite number of time samples [4]. The discrete Fourier transform (DFT) is a special case of the z-transform since it evaluates the z-transform along the $j\omega$ -axis of the s-plane. The FFT has been the backbone of much of the digital signal processing work to date. It is useful in its own right for the spectral information it provides. Perhaps an even more important feature of the FFT is that it can be used as a means to computing numerical convolutions and correlations.

However, the FFT allows us to compute the z-transform along only a very restricted contour. Not only must the contour be the unit circle of the z-plane, output points must be taken uniformly over the entire unit circle. The chirp z-transform (CZT) is an algorithm for computing the z-transform which was developed to overcome these restrictions of the FFT [1]. In Chapter I, the CZT is defined in relation to the general (infinite series) z-transform. Its properties are described and compared with those of the DFT. Then, the computational algorithm for evaluating the CZT is developed using the FFT as its basic component.

In order that the applications might be investigated, a program implementing the CZT was written. Chapter III demonstrates two applications of the CZT: enhancement of poles in spectral analysis, and high resolution narrow-band frequency analysis. Finally, in Chapter IV the report is summarized and a recommendation is made for future work in one possible area of application. An appendix shows a listing of a program in which the CZT appears as a sub-program.

CHAPTER II
THE CHIRP-Z TRANSFORM

2.1 The Z-Transform

The z-transform is a fundamental tool for the analysis of discrete-data systems. It is closely related to the Laplace transform, whose value in studying continuous data systems is well known. In order to see the need for defining the z-transform, consider the discrete function $x^*(t)$ which was obtained by ideally sampling the continuous waveform $x(t)$ every T seconds (see Fig. 2.1). The sequence $x^*(t)$ can be written as

$$x^*(t) = x(t)\delta_T(t) = \sum_{n=0}^{\infty} x(nT)\delta(t - nT), \quad (2 - 1)$$

where $\delta_T(t)$ is a periodic train of unit strength impulses spaced T seconds apart, ie.,

$$\delta_T(t) = \sum_{n=0}^{\infty} \delta(t - nT). \quad (2 - 2)$$

Denoting the Laplace transform of $x^*(t)$ by $X^*(s)$, we obtain

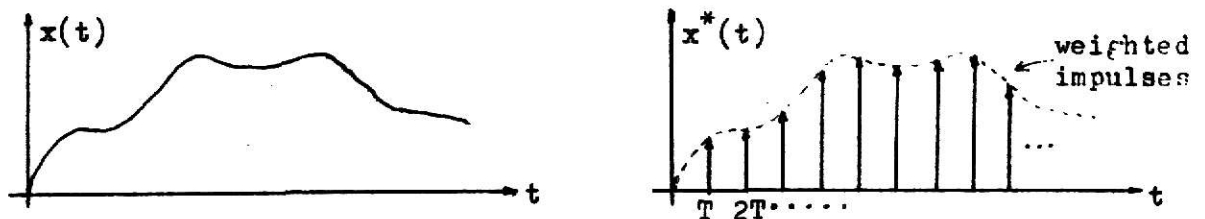
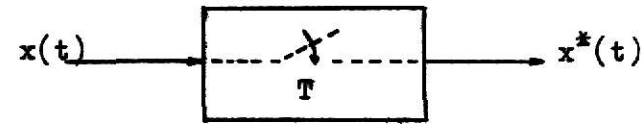
$$X^*(s) = \int_0^{\infty} \left[\sum_{n=0}^{\infty} x(nT)\delta(t - nT) \right] e^{-st} dt \quad (2 - 3)$$

Interchanging the order of integration and summation in Eq. (2-3) and subsequently integrating, there results

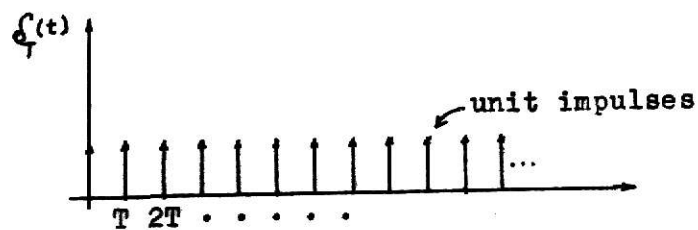
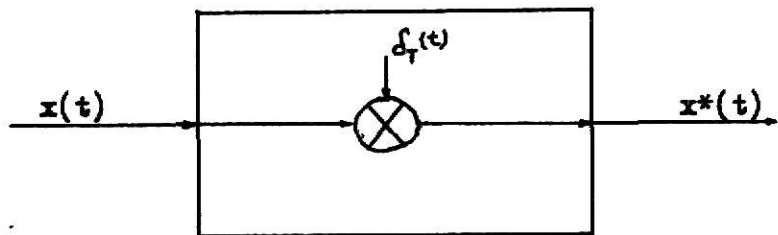
$$X^*(s) = \sum_{n=0}^{\infty} x(nT)e^{-nsT}. \quad (2 - 4)$$

Let us now introduce a new complex symbol

$$z = e^{sT}. \quad (2 - 5)$$



(a) input and output of an ideal sampler



(b) model of an ideal sampler as a multiplication of the input with the impulse train $\delta_T(t)$

Fig. 2-1. The ideal sampling operation.

Therefore from Eq. (2-4) and Eq. (2-5) we have

$$X(z) = \sum_{n=0}^{\infty} x(nT)z^{-n}. \quad (2 - 6)$$

The z-transform of a sequence of numbers x_n is therefore defined as

$$X(z) = \sum_{n=0}^{\infty} x_n z^{-n}. \quad (2 - 7)$$

Note that

$$X(z) \neq [X^*(s)]_{s=z}$$

but that

$$X(z) = [X^*(s)]_{s=(1/T) \ln z}$$

since the s and z-planes are related by the transformation

$$z = e^{Ts} \text{ or } s = (1/T) \ln z.$$

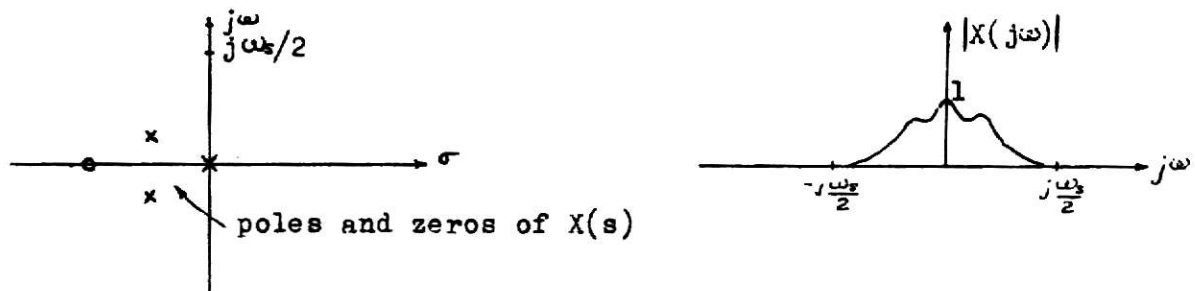
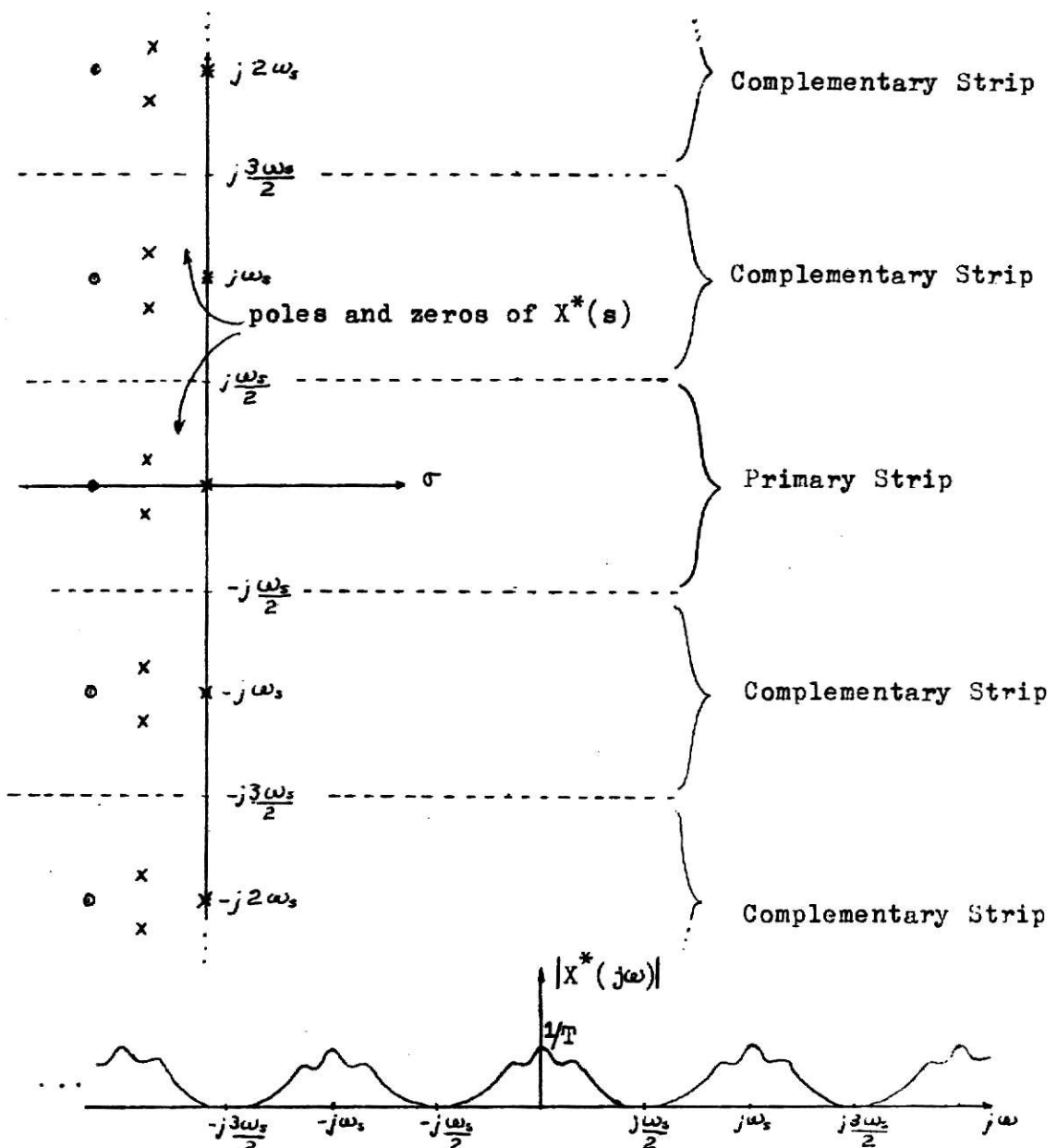
The sampling frequency ω_s is

$$\omega_s = 2\pi/T. \quad (2-8)$$

where T is the time between successive samples (see Fig. 2-1). $X^*(s)$, the Laplace transform of the impulse sequence $x^*(t)$, can be shown to be periodic in the $\text{Im}(s)$ direction with period ω_s (see Fig. 2-2). Figure (2-2b) shows that the ideal sampling operation has the effect of reproducing the frequency spectrum of $X(s)$ in an infinite number of frequency bands in $X^*(s)$. Thus any period (or strip) of $|X^*(j\omega)|$ is identical to $|X(j\omega)|$ except, of course, for a constant factor of $1/T$.

Likewise the transformation $z = e^{sT}$ is periodic with period ω_s . This can be demonstrated by noting that

$$e^{(s+jn\omega_s)T} = e^{sT} e^{jn\omega_s T} = e^{sT} e^{jn2\pi} = e^{sT}$$

(a) continuous function $x(t)$ (b) sampled version of $x(t)$ Fig. 2-2. S-plane representations and Fourier transforms of $x(t)$ & $x^*(t)$

where Eq. (2-8) was used to substitute for ω_s . Thus each strip of $X^*(s)$ maps into the entire z -plane.

It can also easily be shown that the $j\omega$ -axis of the s -plane maps onto the unit circle in the z -plane. Straight lines in the s -plane correspond to logarithmic spirals (in general) in the z -plane. The left half of the s -plane corresponds to the area inside the unit circle and the right half plane corresponds to the area outside the unit circle (see Fig. 2-3). Notice that traversing the $j\omega$ -axis from $-j\omega_s/2$ to $+j\omega_s/2$ is equivalent to one counter clockwise (ccw) revolution around the unit circle starting at $z = e^{j\pi}$.

2.2 Evaluating the Z-Transform of a Finite Sequence

Eq. (2-7) defined the z -transform of a sequence x_n that consisted of an infinite number of points. Since we can only compute $X(z)$ for a finite number of samples, we restrict our attention to sequences with a finite number N of non-zero points. Thus Eq. (2-7) is rewritten as

$$X(z) = \sum_{n=0}^{N-1} x_n z^{-n}. \quad (2 - 9)$$

Even though we have now restricted our attention to the z -transform of a finite sequence x_n , its z -transform $X(z)$ is still a continuous function of z . If the x_n were to be uniform time samples from a known analytic function, then we could in principle find the function $X(z)$. We could then evaluate $X(z)$ for any $z = z_k$ in the z -plane. However, since the x_n with which we are concerned are experimentally obtained, we have no knowledge of the exact analytic function they represent. Thus we cannot obtain the function $X(z)$. We can only calculate the value of the function $X(z)$ at a finite number, say M , of points $z = z_k$. Therefore Eq. (2-9) becomes

ILLEGIBLE DOCUMENT

**THE FOLLOWING
DOCUMENT(S) IS OF
POOR LEGIBILITY IN
THE ORIGINAL**

**THIS IS THE BEST
COPY AVAILABLE**

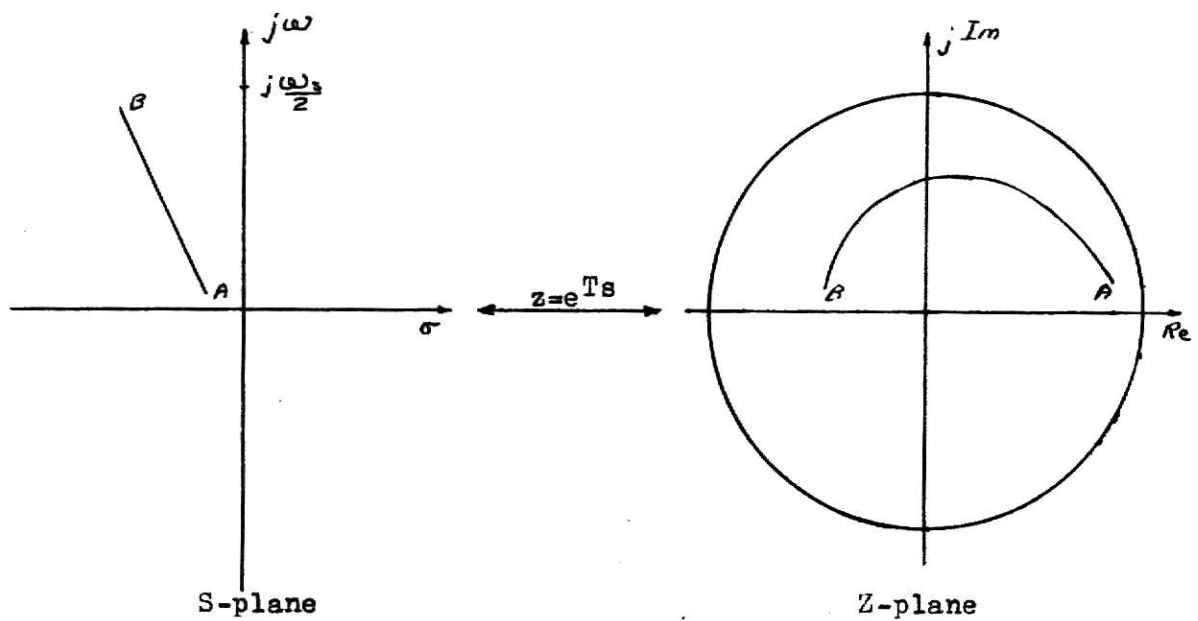
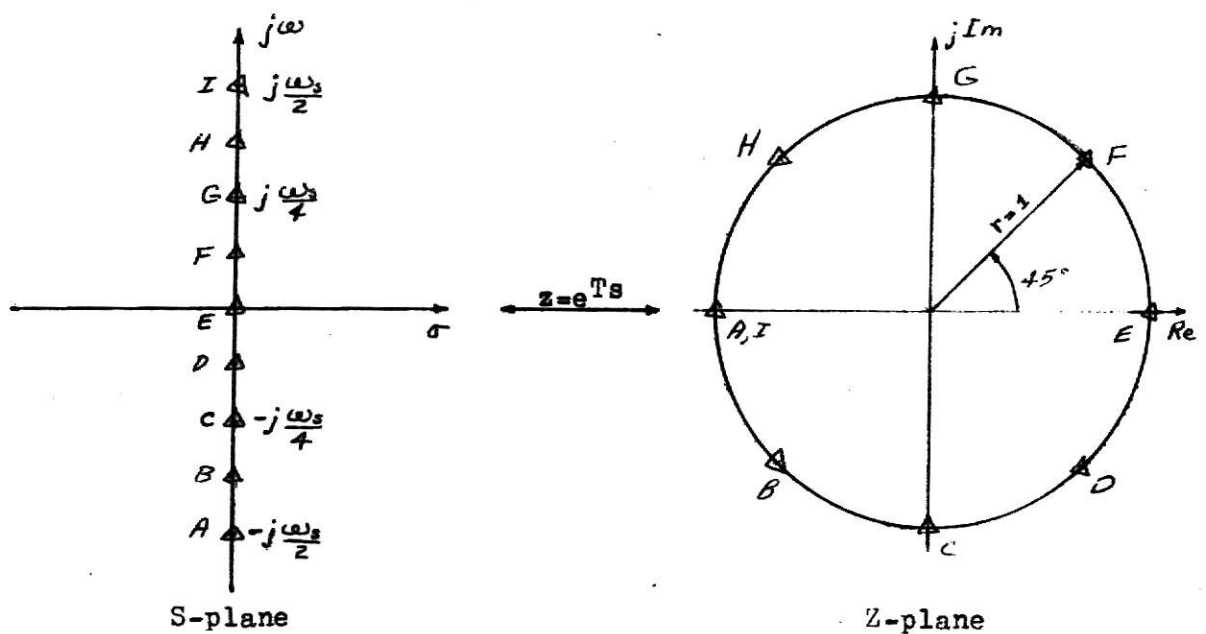


Fig. 2-3. Examples of two contours in both the 'S' & 'Z' planes.

$$x_k = x(z_k) = \sum_{n=0}^{N-1} x_n z_k^{-n} \quad k=0,1,2,\dots,M-1. \quad (2 - 10)$$

Furthermore, for computational reasons that will become apparent later (Sec. 2.4), we shall want to choose the z_k such that all the z_k lie on a particular contour. The general contour that has been chosen is of the form

$$z_k = Aw^{-k}, \quad k=0,1,\dots,M-1 \quad (2 - 11)$$

where M is an arbitrary integer, and A and w are both arbitrary complex numbers of the form

$$A = A_0 e^{j2\pi\theta_0}$$

and

$$w = w_0 e^{j2\pi\phi_0}.$$

Eq.(2-11) describes a set of M points spaced at equal angular increments on a logarithmic spiral. Substituting $z = z_k = Aw^{-k}$ into the relation $s = (1/T) \ln z$, there results

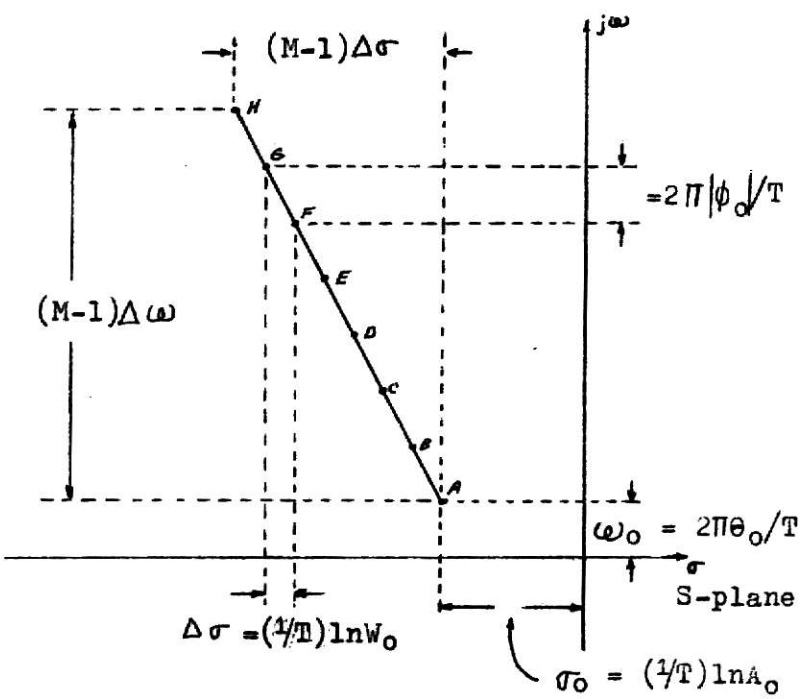
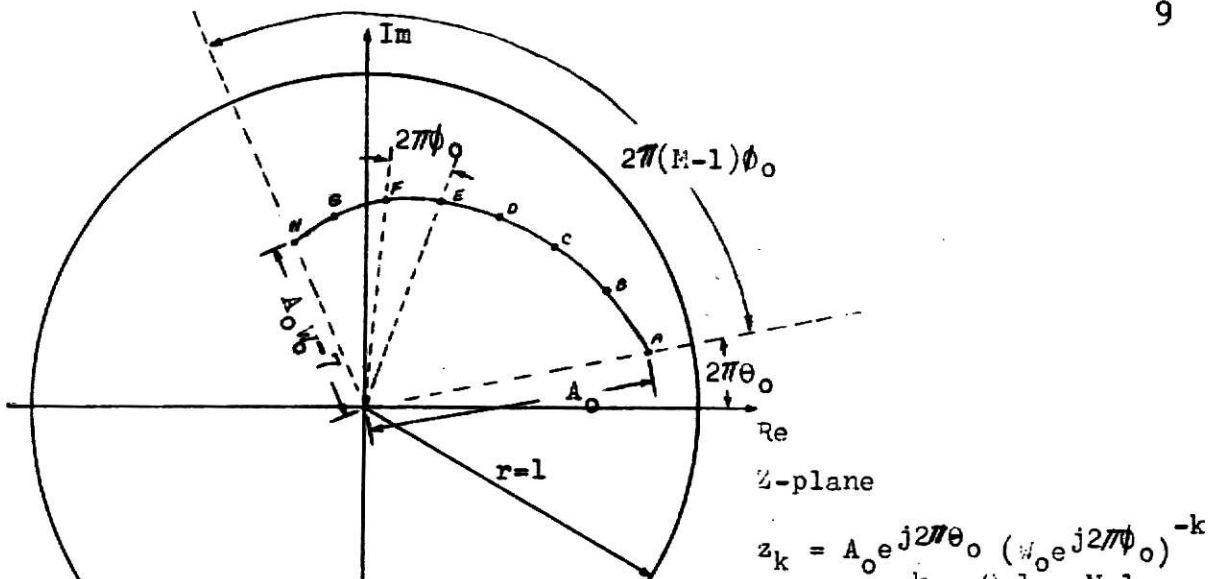
$$s_k = (1/T) \ln A - (k/T) \ln w, \quad k = 0,1,\dots,M-1$$

or

$$s_k = (1/T)(\ln A_0 + j2\pi\theta_0) - (k/T)(\ln w_0 + j2\pi\phi_0).$$

Notice that the z -plane contour maps into a straight line of arbitrary length and orientation in the s -plane. Figure (2-4) illustrates a typical contour of 8 points. Notice that the starting point is completely arbitrary. The contour starts at $z = A_0 e^{j2\pi\theta_0}$ in the z -plane, or correspondingly at $s = (1/T)\ln A_0 + j2\pi\theta_0/T$ in the s -plane.

In order to traverse the contour in the $+j\omega$ direction (s -plane), ϕ_0 must be negative. The frequency spacing in the s -plane (with respect to the $j\omega$ -axis) is equal to $2\pi|\phi_0|/T$ radians/sec., and is arbitrary as are all of the parameters of the contour. Notice also that if $w_0 > 1$,



$$s_k = \left(\frac{1}{T} \ln A_0 + j \frac{2\pi\theta_0}{T} \right) - k \left(\frac{1}{T} \ln \omega_0 + j \frac{2\pi\phi_0}{T} \right)$$

Fig. 2-4. A general CZT contour with $M=8$.

the s-plane contour slopes to the left and vice versa.

Along the general contour that has been chosen, the definition of the z-transform is

$$X_k = X(z_k) = \sum_{n=0}^{N-1} x_n A^{-n} W_0^{kn} \quad k = 0, 1, \dots, M-1. \quad (2 - 12)$$

Equation (2-12) is the form of the z-transform computed by the "Chirp Z-Transform" (CZT) algorithm developed by Rabiner, Schafer, and Rader [1].

2.3 A Special Case of the CZT

If we let $A_0 = 1$, $\theta_0 = 0$, $W_0 = 1$, $M = N$, and $\phi_0 = -1/N$; then Eq. (2-12) becomes

$$X(z_k) = \sum_{n=0}^{N-1} x_n e^{-j(2\pi/N)nk} \quad k = 0, 1, \dots, N-1. \quad (2 - 13)$$

Equation (2-13) is known as the discrete Fourier transform (DFT). The DFT is sometimes defined as

$$X(z_k) = \frac{1}{N} \sum_{n=0}^{N-1} x_n e^{-j(2\pi/N)nk} \quad k = 0, 1, \dots, N-1$$

where the only difference is seen to be the addition of a constant multiplier. Equation (2-13) is used to define the DFT in this paper as it is consistent with the definition of the more general z-transform.

The contour of evaluation for the DFT is seen to be the unit circle of the z-plane or the $j\omega$ -axis in the s-plane. The points of evaluation along the $j\omega$ -axis are equally spaced at

$$\omega = \frac{2\pi k \phi_0}{T} = \frac{2\pi k}{T} \frac{1}{N} \quad k = 0, 1, \dots, N-1.$$

For example, consider the case where $N = 8$. Then

$$\Delta\omega = \frac{2\pi}{T} \frac{1}{8} = \frac{\omega_s}{8}.$$

The points of evaluation of the z-transform by the DFT are illustrated for this example in Fig. (2-5). Notice that the evaluation points are harmonically related to ω_s/N , and that they are equally spaced around the entire unit circle. Due to this characteristic of the DFT, we could not evaluate the z-transform at $\omega = 3\omega_s/16$ without also evaluating it at

$$\omega = k(\omega_s/16) \quad k = 0, 1, 2, \dots, 15.$$

In other words, to double the frequency resolution in one small interval of the unit circle, we would have to double it around the entire unit circle. This handicap is overcome by the flexibility of the CZT. This feature of the CZT will be demonstrated in Chapter III.

The DFT became very popular after 1965 when Cooley and Tukey first developed the Tukey-Cooley algorithm for rapidly computing the DFT [4]. This algorithm is generally referred to as the fast Fourier transform (FFT).

The FFT allows computation of the DFT with computational time and storage requirements proportional to $N \log_2 N$ when N is a power of two. Direct solution of the $(N \times N)$ equations implied by Eq. (2-13) would require time and storage proportional to N^2 .

The FFT requires $\log_2 N$ iterations, with each iteration consisting of N additions (or subtractions) and N multiplications. Figure 2-6 shows the FFT signal flow graph when $N = 8$. Appendix A contains a listing of a FORTRAN program that implements the FFT algorithm.

2.4 Computation of the CZT

In review, the CZT was defined as the z-transform of the N -point

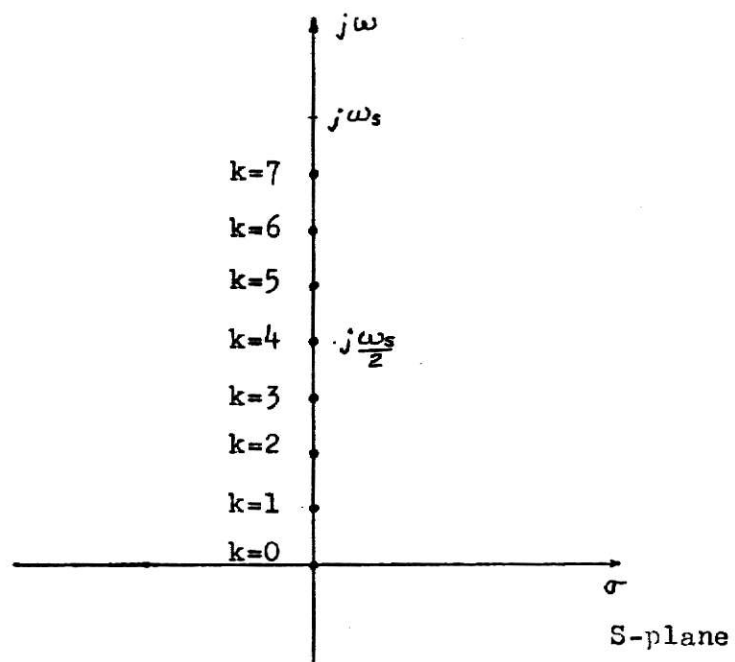
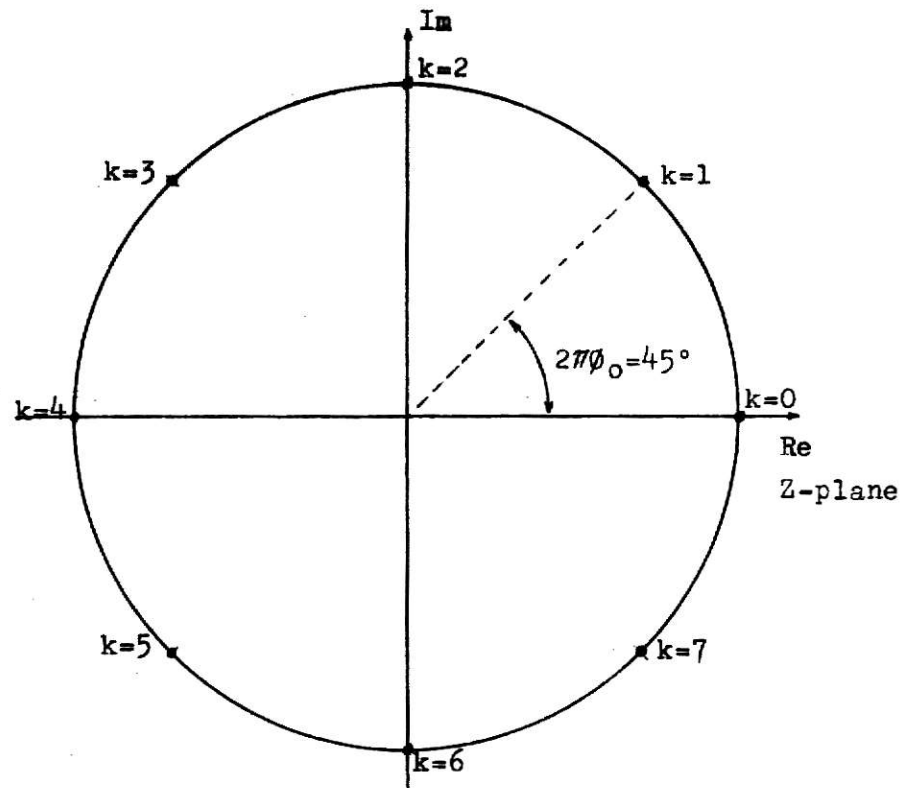
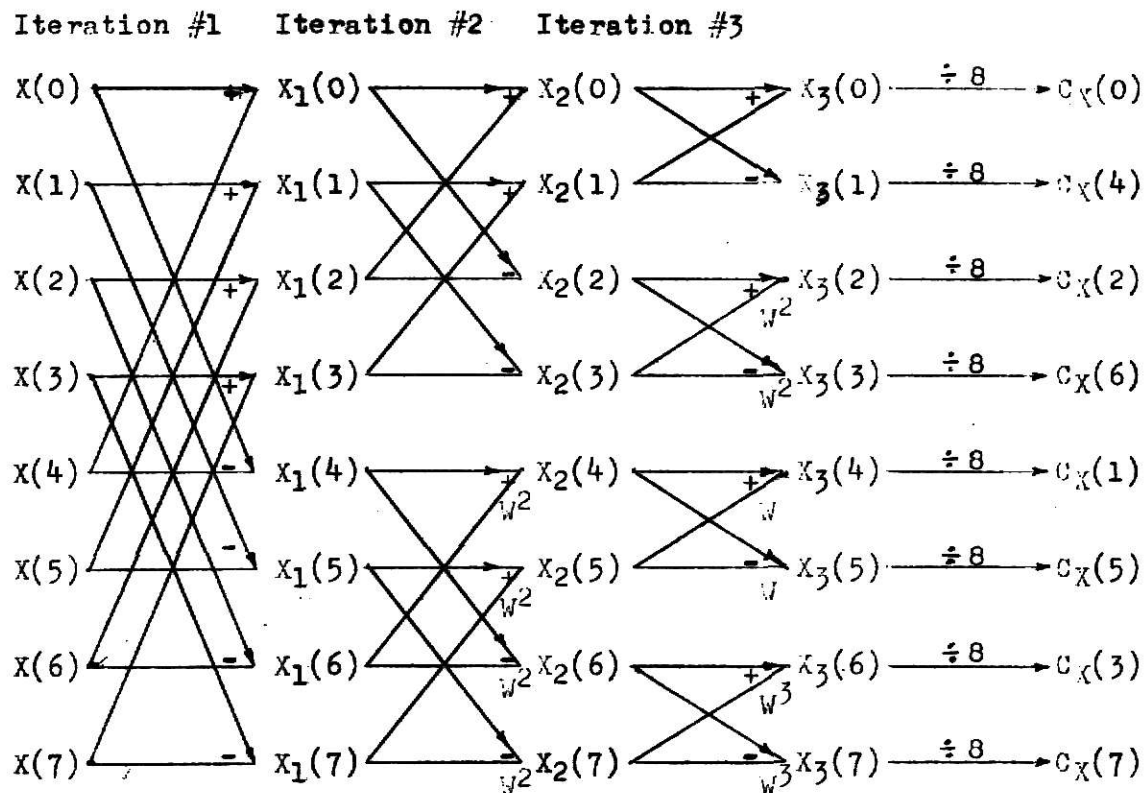


Fig. 2-5. Contour for an 8-point FFT.



$$\text{where } w = e^{-j2\pi/N} = e^{-j\pi/4}$$

Notation:

$$x_j(p) \xrightarrow{\alpha} x_{j+1}(p) = x_j(p) + \alpha x_j(q)$$

$$x_j(q)$$

$$x_j(p)$$

$$x_j(q) \xrightarrow{-\alpha} x_{j+1}(q) = x_j(p) - \alpha x_j(q)$$

NOTE: The definition of the FFT used in the Fortran program listed in Appendix A does NOT include the multiplication factor of $1/N$, located after the last iteration in the standard flow graph.

Fig. 2-6. Standard FFT signal flow graph, $N=8$.

sequence x_n . Furthermore, we said we would restrict the computation of the CZT to M points along the contour

$$z_k = AW^{-k} \quad k = 0, 1, \dots, M-1.$$

Therefore we defined the CZT in Eq. (2-12) as

$$x_k = X(z_k) = \sum_{n=0}^{N-1} x_n A^{-n} W^{nk} \quad k = 0, 1, \dots, M-1. \quad (2 - 12)$$

Equation (2-12) indicates that a straight forward solution of the $N \times M$ system of equations would require a number of arithmetic operations proportional to NM . Thus the short cuts that led to computing the DFT via the FFT do not appear to exist in the CZT. This indeed would have been the only alternative if the z_k had not been systematically chosen. However, let us now make the substitution, due to Bluestein [5]

$$nk = \frac{n^2 + k^2 - (k-n)^2}{2}$$

for the exponent of W in Eq. (2-12). This equation then becomes

$$x_k = \sum_{n=0}^{N-1} x_n A^{-n} W^{(n^2/2)} W^{(k^2/2)} W^{-(k-n)^2/2} \quad k = 0, 1, \dots, M-1. \quad (2 - 14)$$

The factor $W^{-(k-n)^2/2}$ in Eq. (2-14) suggests that Eq. (2-14) may be considered to involve a discrete convolution. Recall that the convolution of the discrete sequences $r(n)$ and $s(n)$ is

$$r(n) * s(n) = t(k) = \sum_{n=0}^k r(n)s(k-n)$$

or

$$t(k) = \sum_{n=0}^k s(n)r(k-n) \quad k = 0, 1, 2, 3, \dots$$

Therefore, Eq. (2-14) can be looked upon as a three step process consisting of:

- (1) forming a new sequence y_n by weighting the x_n according to the equation

$$y_n = x_n A^{-n} W^{n^2/2} \quad n = 0, 1, \dots, N-1, \quad (2 - 15)$$

- (2) convolving y_n with the sequence v_n defined as

$$v_n = W^{(n^2/2)} \quad (2 - 16)$$

to give a sequence g_k

$$g_k = \sum_{n=0}^{N-1} y(n)v(k-n) \quad k = 0, 1, \dots, L-1, \quad (2-17)$$

- (3) and multiplying g_k by $W^{k^2/2}$ to give

$$x_k = g_k W^{k^2/2} \quad k = 0, 1, \dots, M-1. \quad (2 - 18)$$

This process, the CZT algorithm, is illustrated in the block diagram shown in Fig. (2-7). Steps (1) and (3) require N and M complex multiplications respectively. The most time consuming part of the CZT is step (2), the convolution.

The practicality of the CZT depends upon having available a high speed method of computing the discrete convolution. The fastest technique available for computing a discrete convolution involves using the FFT. Recall that the product of the DFT's of two sequences is the DFT of the circular (periodic) convolution of the two sequences. Therefore we may compute the sequence g_k (see Fig. 2-8) by:

- (1) Using the FFT to compute the DFT of y_n , call it Y_r .

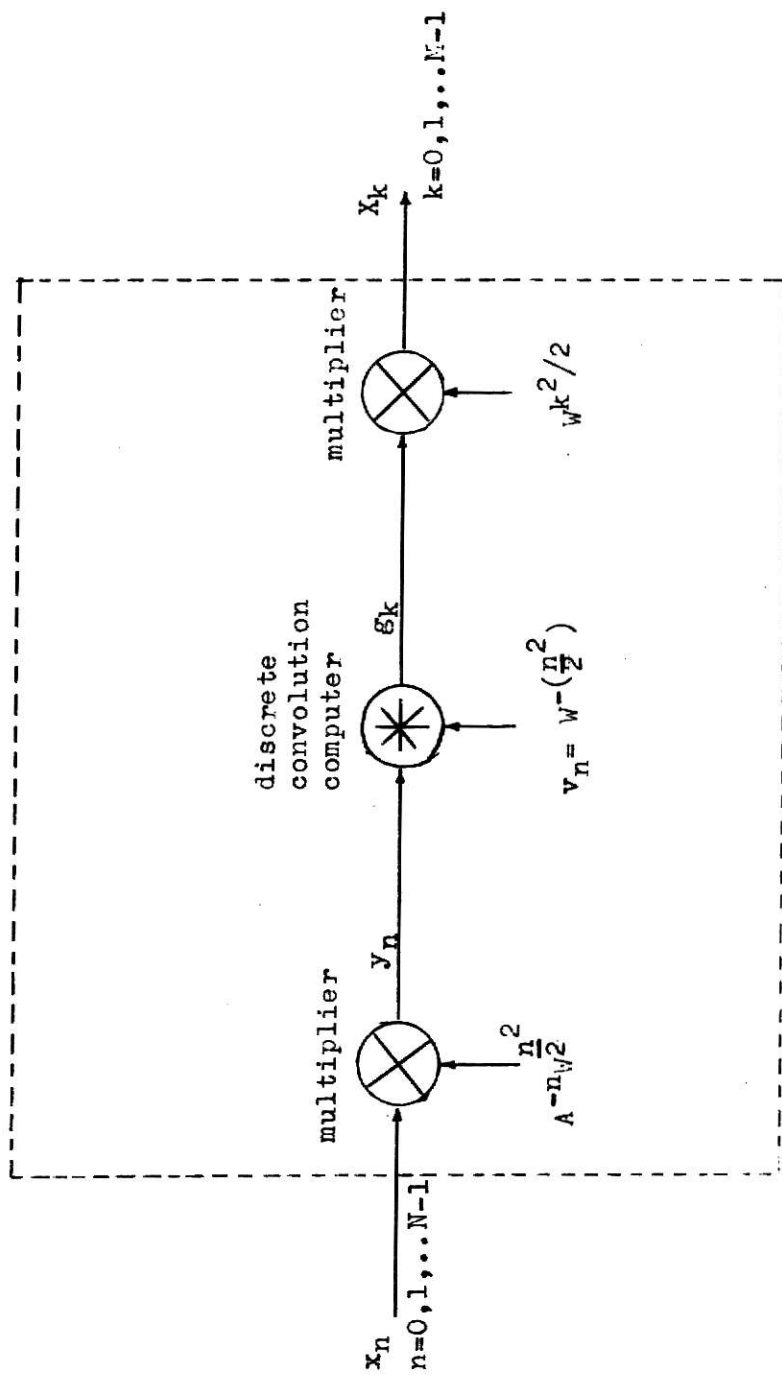


Fig. 2-7. An illustration of the steps in the CZT algorithm.

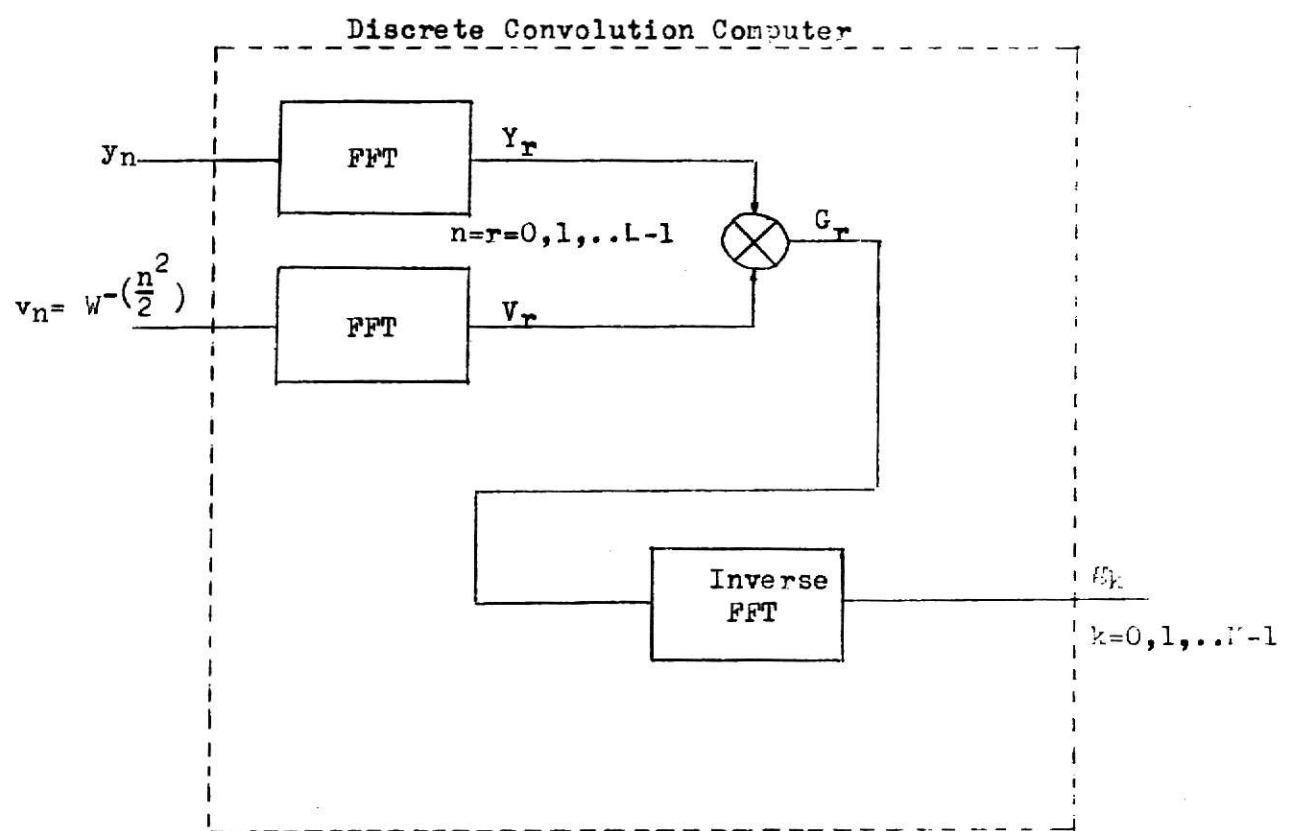


Fig. 2-8. Block diagram of the way the FFT is used in computing the convolution in the CZT.

(2) using the FFT to compute the DFT of v_n , call it V_r .

(3) multiplying V_r and V_r to yield G_r

(4) using the FFT to compute the inverse DFT of G_r , ie., g_k .

The resulting sequence g_k is one period of the periodic convolution of y_n and v_n . Unless we artificially lengthen one or both of the sequences y_n and v_n , adjacent periods in the convolution sequence will overlap. Thus we will extend each sequence by appending zeros such that the total length of each will be L samples. L must be greater than or equal to $(M + N - 1)$. Therefore the resulting sequence g_k will be the same as an ordinary (aperiodic) convolution.

In summary, the CZT algorithm consists of the following steps.

- (1) Choose L to be the smallest integer which is a power of two and is greater than or equal to $(M + N - 1)$. The power of two requirement is imposed by the available FFT program.
- (2) Form an L point sequence y_n from x_n by weighting the x_n according to

$$y_n = \begin{cases} A^{-n} W^{n^2/2} x_n & n = 0, 1, 2, \dots, N-1 \\ 0 & n = N, N+1, \dots, L-1. \end{cases} \quad (2 - 19)$$

- (3) Compute the L point DFT of y_n , calling it V_r , $r = 0, 1, \dots, L-1$.
- (4) Form the L point sequence v_n from the indefinite length sequence $w^{-(n^2/2)}$ by the equation

$$v_n = \begin{cases} w^{-(n^2/2)} & 0 \leq n \leq M-1 \\ 0 & M-1 < n < L-N+1, \text{ if } L > M+N-1 \\ w^{-(L-n)^2/2} & L-N+1 \leq n \leq L-1. \end{cases} \quad (2 - 20)$$

Note that if $L = M + N - 1$, there will be no terms in v_n equal to zero. The sequence v_n is defined in this peculiar manner in order to make the periodic convolution conveniently yield the desired ordinary convolution.

- (5) Compute the L point DFT of v_n , calling it V_r , $r = 0, 1, \dots, L-1$.
- (6) Multiply the sequences Y_r and V_r , yielding $G_r = Y_r V_r$, $r = 0, 1, \dots, L-1$.
- (7) Compute the L point IDFT of G_r , calling it g_k , $K = 0, 1, \dots, L-1$.
- (8) Multiply the first M terms of g_k by $w^{k^2/2}$ yielding

$$x_k = w^{k^2/2} g_k, \quad k = 0, 1, \dots, M-1.$$

CHAPTER III

APPLICATION CONSIDERATIONS

3.1 Enhancement of Poles

Recall that one of the features of the CZT is its ability to evaluate the z-transform along a logarithmic spiral contour in the z-plane. In contrast, the DFT evaluates the z-transform only on the unit circle. This feature of the CZT is of value in precisely locating the poles and zeros of a system transfer function. The distance of a pole from the real axis in the s-plane can be approximately determined from the peak the pole produces in the system frequency response plot.

The sharpness of a resonant peak varies inversely with the distance between the $j\omega$ -axis and the pole. Therefore the sharpness of a resonance peak can be enhanced by evaluating the z-transform along a contour that lies closer to the pole(s) than the contour for the DFT, the $j\omega$ -axis. To demonstrate this feature, consider the following example (see Fig. 3-1). Figure (3-1) depicts a simple system with only one complex pole pair. The system's impulse response was simulated by evaluating the function

$$e_n = e^{-4n\Delta t} \cos(2\pi)4n\Delta t \quad n = 0, 1, \dots, 63. \quad (3 - 1)$$

The sampling interval, Δt , was chosen to be >8 Hz. in order to satisfy the Nyquist sampling requirement. The CZT of the sequence e_n , $n = 0, 1, \dots, 63$, was evaluated along four contours, each parallel to the $j\omega$ -axis. The resulting CZT's are plotted in Fig. (3-2). Notice that there is a marked increase in the sharpness of the resonant peaks as the evaluation contour is moved closer to the pole. Thus the presence of poles can be made to stand out and their frequencies determined more accurately using the CZT with an appropriate CZT rather than with the DFT.

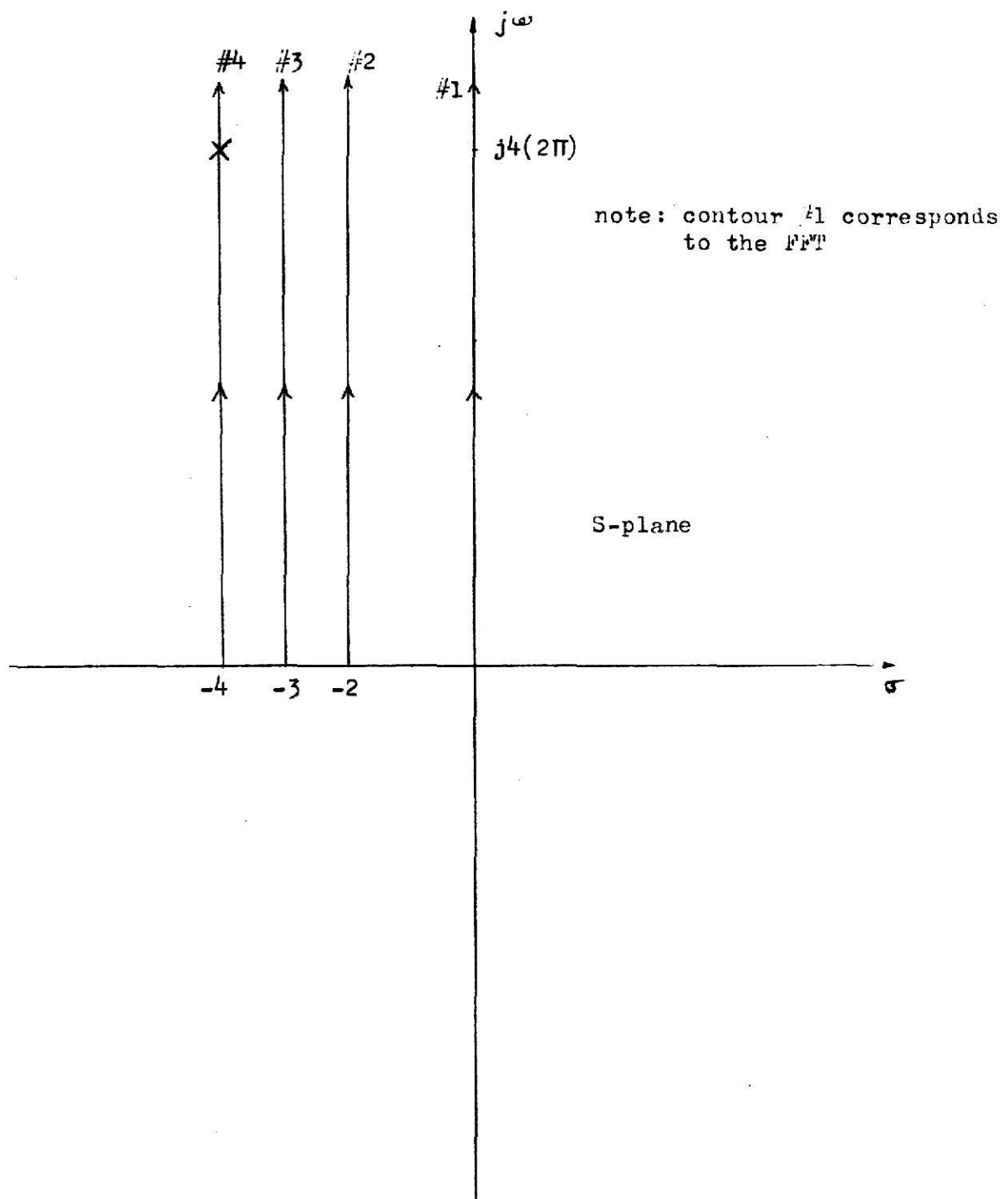


Fig. 3-1. Four contours used to show the effect of moving the CZT contour closer to the pole.

12-189
12-189

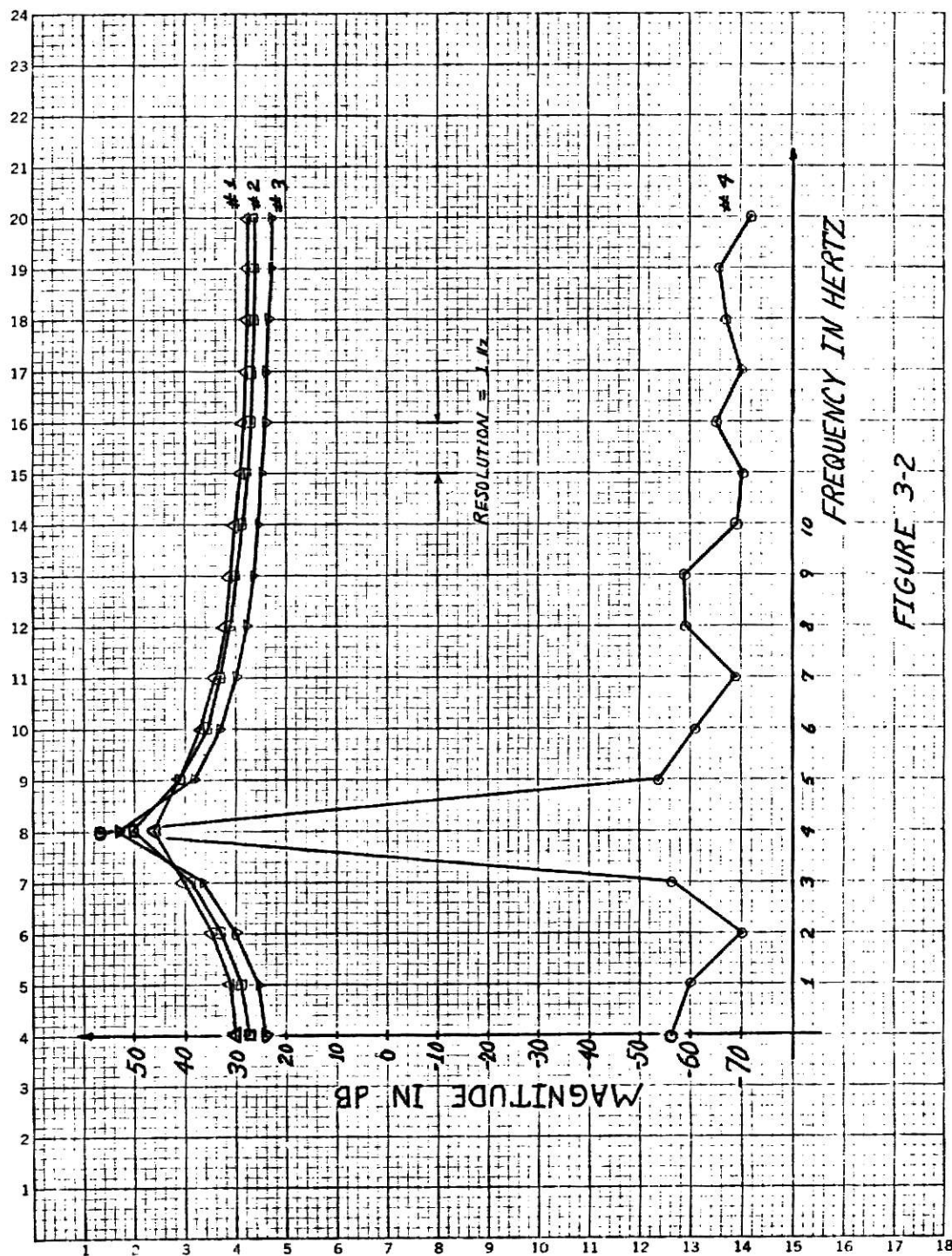


Fig. 3-2. Example of pole enhancement using four different CZT contours.

Speech analysis is a field that may be able to utilize this property of the CZT [6,7,8]. For example, voiced speech can be modeled by a time-varying linear system, whose impulse response varies with the configuration of the vocal tract. The vocal tract impulse response is basically the sum of 3 to 5 damped sinusoids, i.e., 3 to 5 complex pole pairs. The location of the formants (or poles) depends on the particular voiced sound being made. The CZT is one method that may aid speech researchers in automatically detecting and tracking these time-varying formants. Using the CZT to implement a formant tracking vocoder is being studied [1,8]. Since the CZT can be used to sharpen the resonant peaks, the formant frequencies could be determined more accurately with an appropriate CZT contour than they could with the FFT. A simple example of a system that has pole locations similar to those of the human vocal tract is shown in Fig. (3-3). Figure (3-3) shows the poles of a system with a transfer function

$$H(s) = \frac{1}{(s^2 + 160s + 256400)(s^2 + 100s + 3242500)(s^2 + 80s + 4411600)} \quad (3 - 2)$$

where s is in Hertz.

Since the highest frequency component in the system impulse response is 2100 Hz., the sampling frequency, $1/T$, was chosen to be 5000 Hz. The CZT contour was chosen to pass through the origin and the point $s = -40 + j2000$ Hz. The contour parameters for the CZT program were calculated as follows:

$$\text{set } \omega_0 = 0 = \frac{2\pi\theta_0}{T} \Rightarrow \theta_0 = 0$$

$$\text{set } \sigma_0 = 0 = (1/T) \ln A_0 \Rightarrow A_0 = 1$$

$$\text{set } |\Delta\omega| = \frac{2500(2\pi)}{64} = \frac{2\pi\phi_0}{T} \Rightarrow \phi_0 = -1/128$$

(ϕ must be negative in order to move along the contour in the desired direction)

$$\text{set } \frac{\Delta\omega}{\Delta\sigma} = \frac{-2000}{40} = \frac{2\pi\phi_0}{\ln W_0} \Rightarrow W_0 = \exp[2\pi/6400]$$

Figure (3-4) shows a plot of $|H(j\omega)|^2$ as computed by the 64 point FFT. The FFT resolution is $f_0 = 78.125$ Hz. ($f_0 = 1/NT = 5000/64$). Figure (3-5) shows a plot of $|H(s)|^2$ as evaluated by the CZT along the prescribed contour off the $j\omega$ -axis. The 64 point CZT resolution was chosen to be 39.0625 Hz., exactly twice that of the FFT. Only every other point of the CZT output was plotted in Fig. (3-5) so that the resolution would be the same as that for the FFT plot (Fig. 3-4). Note that the poles produce somewhat narrower peaks in the CZT plot (Fig. 3-5) than they do in the FFT plot. Figure (3-6) shows the CZT plot with every point plotted giving a resolution of 39.0625 Hz. Increasing the resolution of the CZT beyond that given by the FFT begins to reveal the ripples in the z-transform which result from using only a finite number of data samples. The low resolution CZT appears to accentuate the poles better than does the relatively higher resolution CZT.

Thus the CZT does make some improvement in sharpening the resonances due to the poles. Several examples of using the CZT in this manner are shown in the paper on the CZT by Rabiner, Schafer, and Rader [1].

3.2 High Resolution, Narrow Band Spectra

Recall that a second feature of the CZT was the arbitrary starting point of the contour. The arbitrary starting point of the contour is not unique to the CZT. The FFT contour can be started at a point $z = |A|e^{j2\pi\theta_0} = A$ by simply multiplying the data sequence x_n , $n = 0, 1, \dots, (N-1)$ by A^{-n} [1]. However, this capability with the FFT is not of much value since we can only shift the starting point by $0 \leq \theta_0/T \leq f_0$, ($f_0 = (1/NT)$ Hz.). The term (θ_0/T)

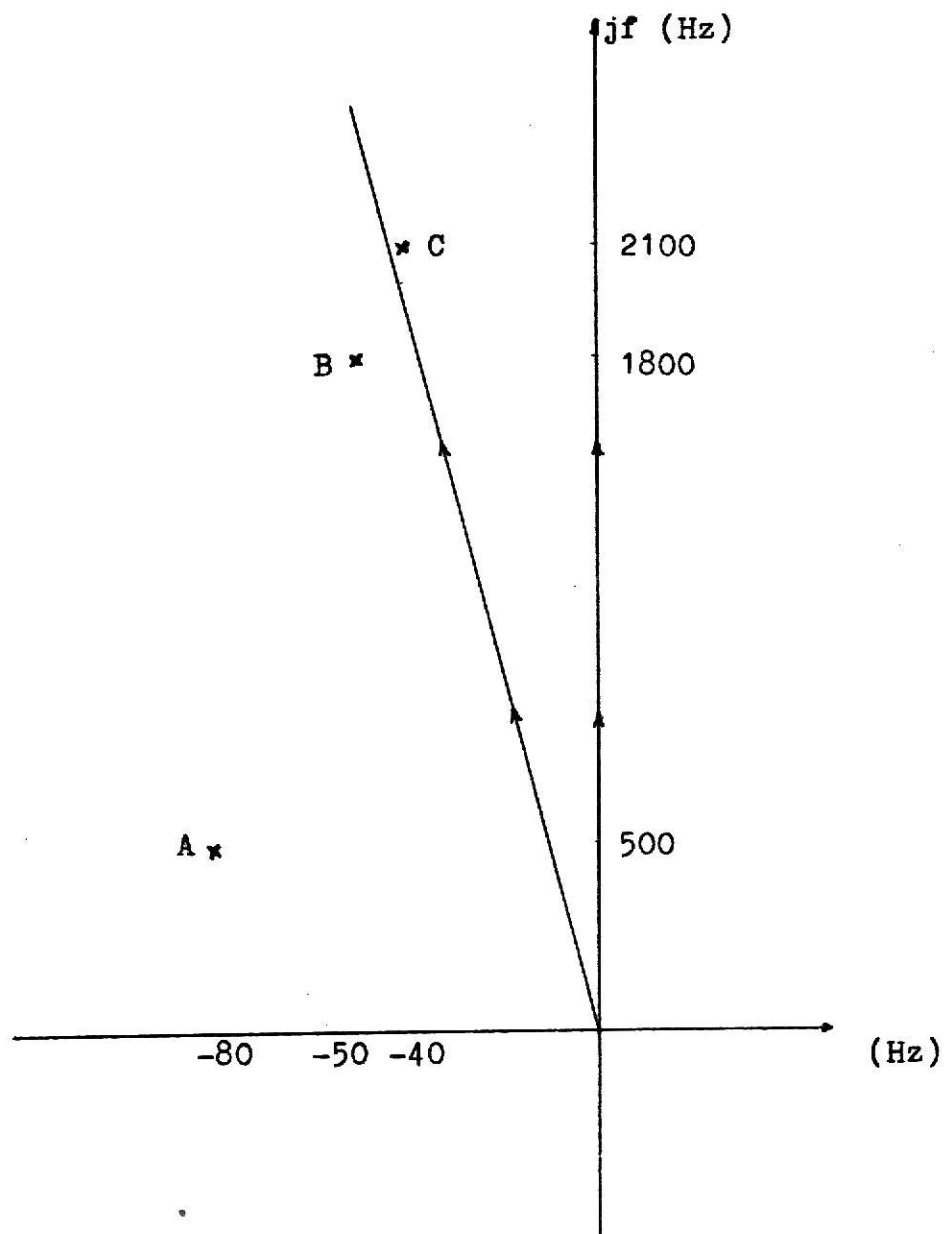


Fig. 3-3. FFT and CZT contours for a three pole system.

12-189
12-189

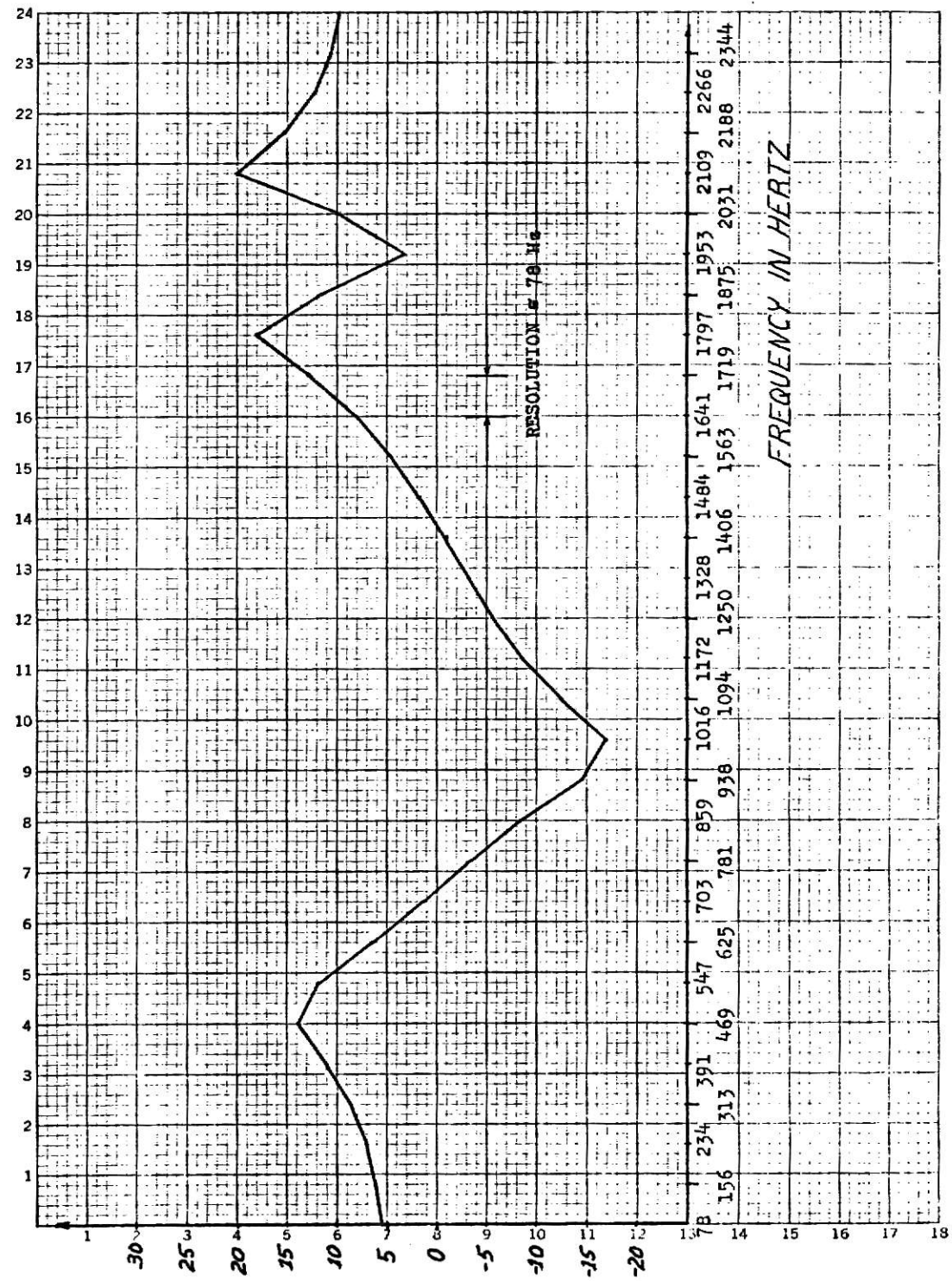


Fig. 3-4. $|H(j\omega)|^2$ as computed by the FFT (78 Hz. resolution).

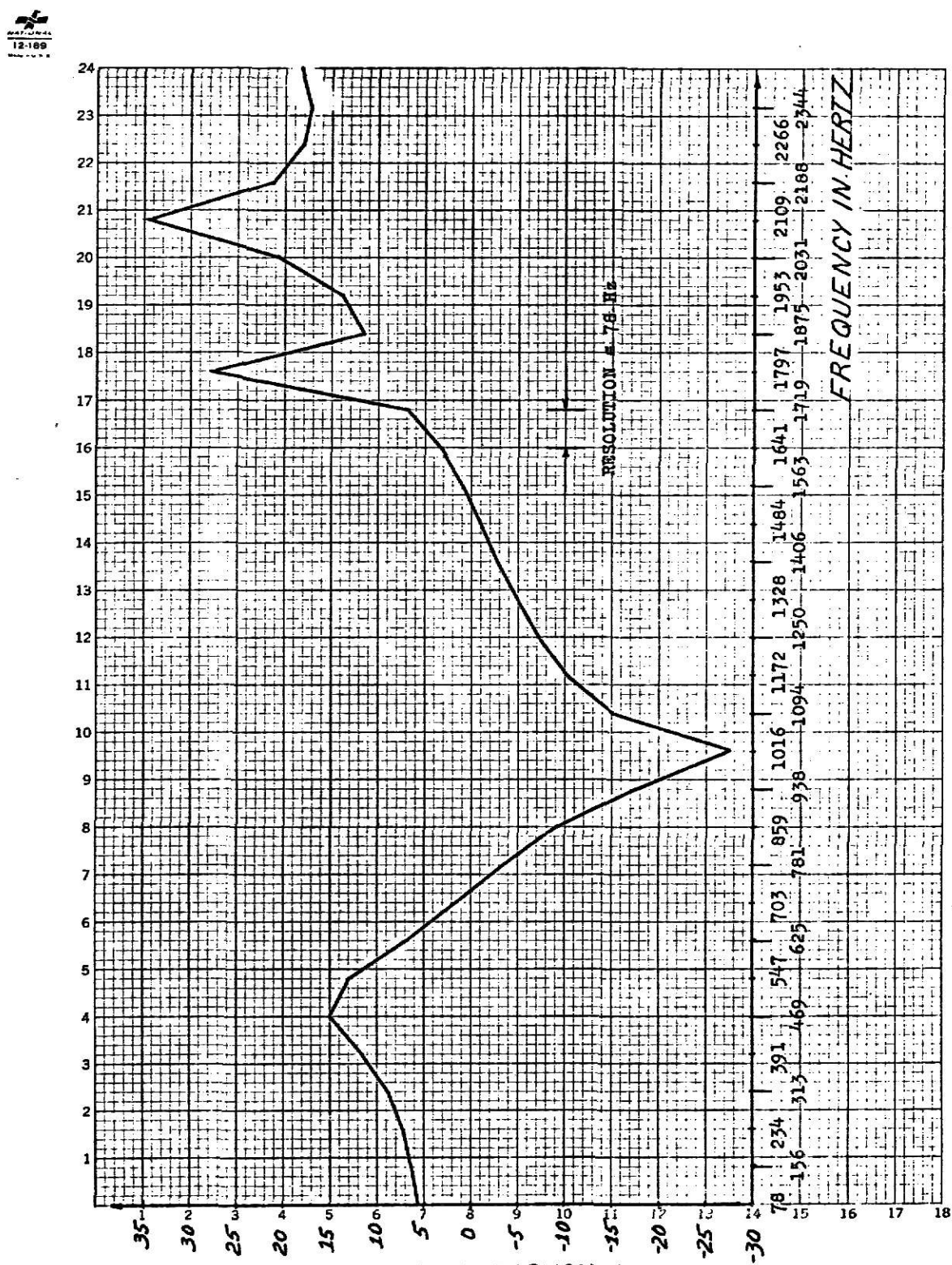


Fig. 3-5. $|H(s)|^2$ as computed by the CZT (78 Hz. resolution).

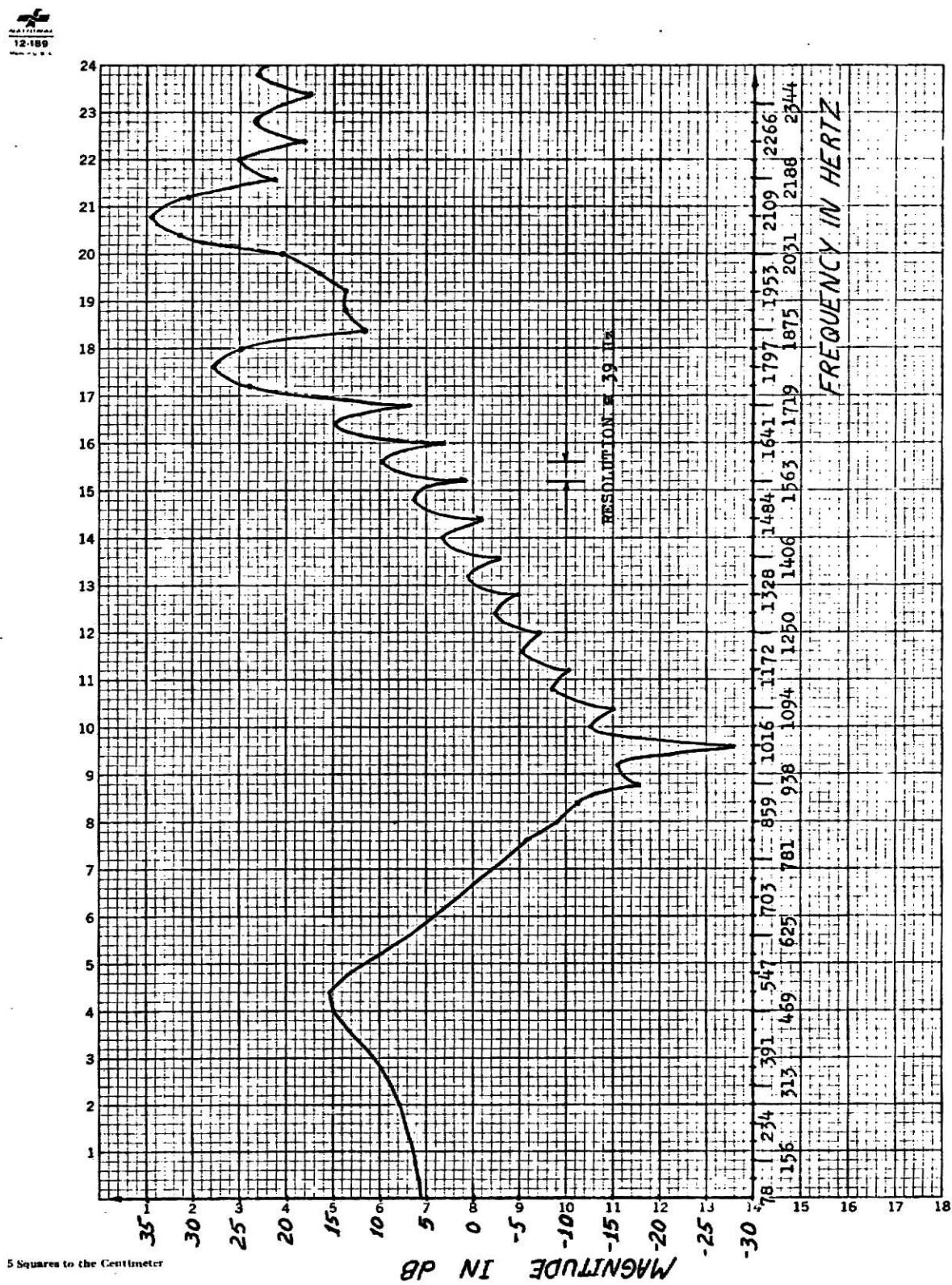
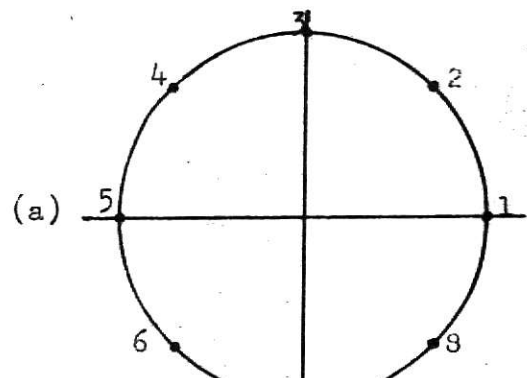


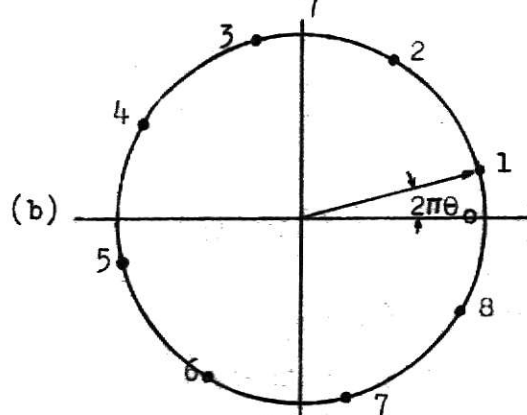
Fig. 3-6. $|H(s)|^2$ as computed by the CZT (39 Hz. resolution).

is limited to f_0 Hertz because the FFT evaluates the z-transform once around the unit circle and the z-transform is periodic around the unit circle. This is best explained by considering the four 8-point FFT's shown in Fig. (3-7). Part (a) shows a conventional FFT starting at $z = e^{j0}$. In part (b), x_n , $n = 0, 1, \dots, 7$ has been multiplied by $e^{-j2\pi\theta_0 n}$, $\theta_0/T < f_0$, prior to computing the FFT. Figure (3-7c) shows the result of setting $\theta_0/T = f_0$. It is clear that (c) is really the same as (a). Likewise setting $\theta_0/T = 2.5f_0$ in (d) is equivalent to $\theta_0/T = (n+0.5)f_0$, $n = 1, \pm 1, \pm 2, \dots$. Therefore the starting point for the FFT can indeed be shifted, but the maximum shift is limited to $f_0 = 1/NT$ Hz. which is the resolution of the FFT.

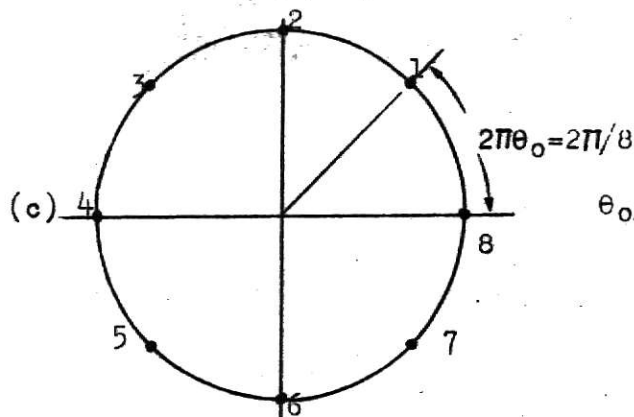
In contrast, the CZT contour starting point can be moved (from $z = e^{j0}$) by an amount $2\pi\theta_0$, $0 \leq \theta_0/T < f_s$ ($f_s = 1/T$ Hz.). This shift is meaningful since, unlike the FFT, we are not constrained to a contour that traverses the entire unit circle. Thus a second important feature of the CZT is that we are completely free to choose the frequency spacing of the contour, independent of N and T. Using the CZT, the z-transform may be evaluated only along an arc of the unit circle. This means that the CZT allows us to obtain spectral information only over a band of frequencies within the range $0 \leq f < f_s$. Consider the standard 8-point FFT contour shown in Fig. (3-8a). Only points 1 through 5 on the contour of Fig. (3-7a) are independent. Points 6 through 8 are just the conjugates of 4 through 2, respectively. Therefore points 6 through 8 are of little value since we could just as easily have constructed them ourselves from points 4 through 2. By using the CZT to evaluate the z-transform on the unit circle, we could cover the same "useful" frequency range, $0 \leq f \leq f_s/2$, with the resolution improved by a factor of 2 with just nine output points (see Fig. 3-8b). Or, if we were really only



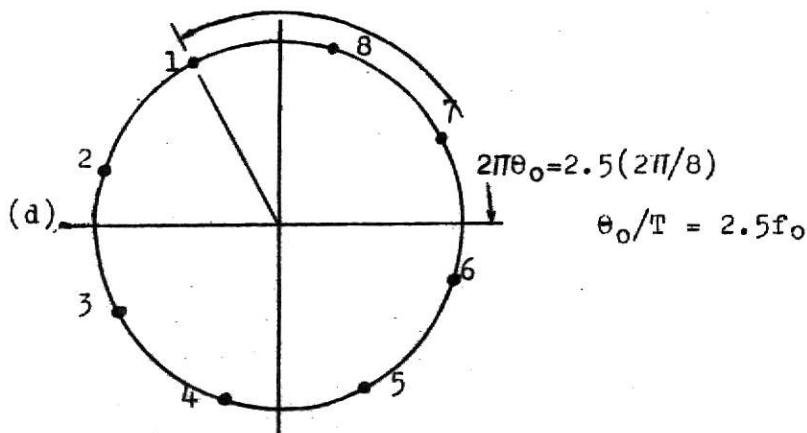
T = time between successive samples



$\theta_0/T < f_0$ (where $f_0=1/T$ is fundamental freq. of the FFT.)



$$\theta_0/T = f_0$$



$$\theta_0/T = 2.5f_0$$

Fig. 3-7. Frequency shifted FFTs ($N=8$).

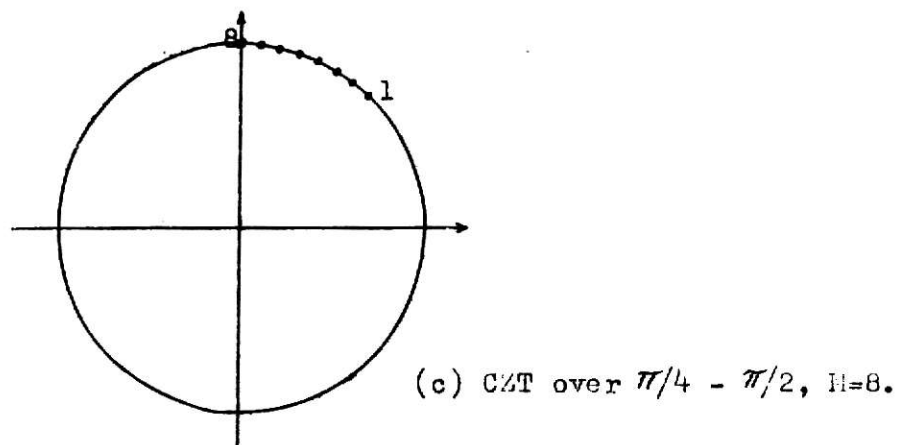
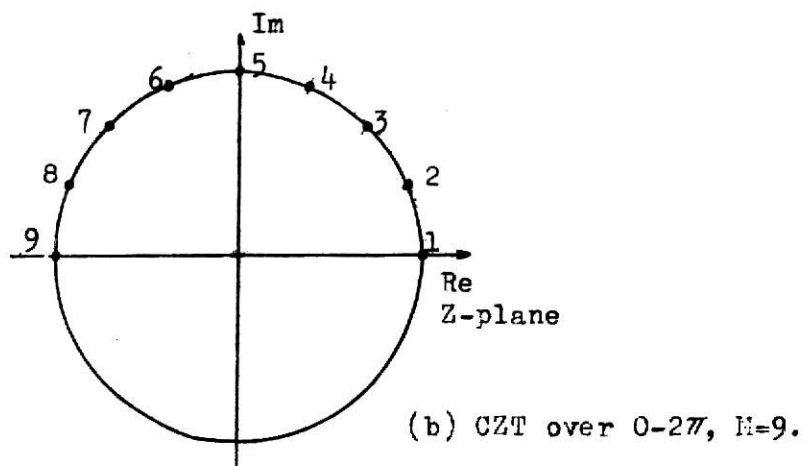
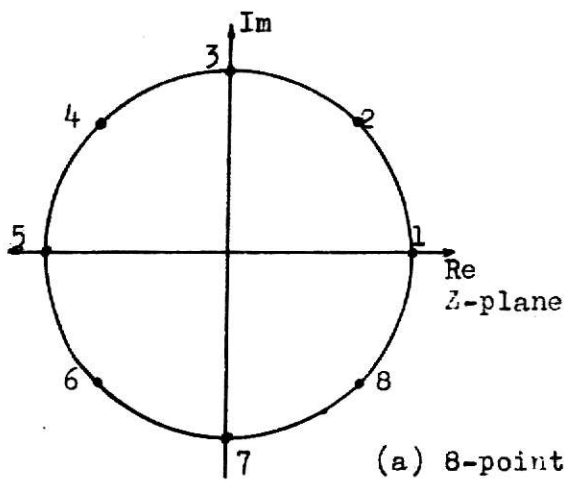


Fig. 3-8. Examples of FFT and CZT contours.

interested in the range $\pi/4 < 2\pi\theta < \pi/2$, the CZT would allow us to evaluate the contour in Fig. (3-8c).

The CZT is thus a much more efficient means of obtaining high resolution band spectra than is the FFT. One application of this capability could be in the analysis of the frequency responses of digital filters. Consider the following simulated simple bandpass filter [1].

$$h(nT) = \sin[\pi(F_2 + F_1)(n-m-1/2)T] \cos[\pi(F_2 - F_1)(n-m-1/2)T]$$

$$0 \leq n < 2m \quad (3 - 3)$$

where

$2m$ = number of terms in truncated impulse response = 64

$1/T$ = sampling frequency = 10,000 Hz.

F_1 = lower cutoff frequency = 900 Hz.

F_2 = upper cutoff frequency = 1100 Hz.

$h(nT)$ is the sampled version of a symmetrically truncated impulse response of a bandpass filter. The function $h(nT)$ is plotted in Fig. (3-9). Evaluating the z-transform of $h(nT)$ along the unit circle yields the frequency response of the filter. Figure (3-10) shows the frequency response computed from a 64-point FFT. The resolution is

$$f_o = \frac{1}{NT} = \frac{4}{64} = 156.25 \text{ Hz.}$$

Notice that this FFT gives us little information about the passband of the filter. Figure (3-11a) shows the CZT frequency response of the filter in the range $500 \leq f \leq 1460$ Hz, with a resolution of 15 Hz. Given a fixed sampling rate, we could improve the resolution of the FFT by adding zeros to the end of the impulse response sequence, thus artificially decreasing f_o .

Adding 448 zeros would have yielded a 512 point FFT with resolution $f_0 \approx 20$ Hz.
 $(f_0 = 1/512T = 10^4/512)$.

If we compare the amount of calculations required, we see that the 64 output point CZT requires three 128 point FFT's to be computed. In contrast the 512 point FFT would have required approximately 60% more computer time. This is assuming:

$$\text{time to calculate CZT} \approx \beta(3)128 \log_2 128$$

and

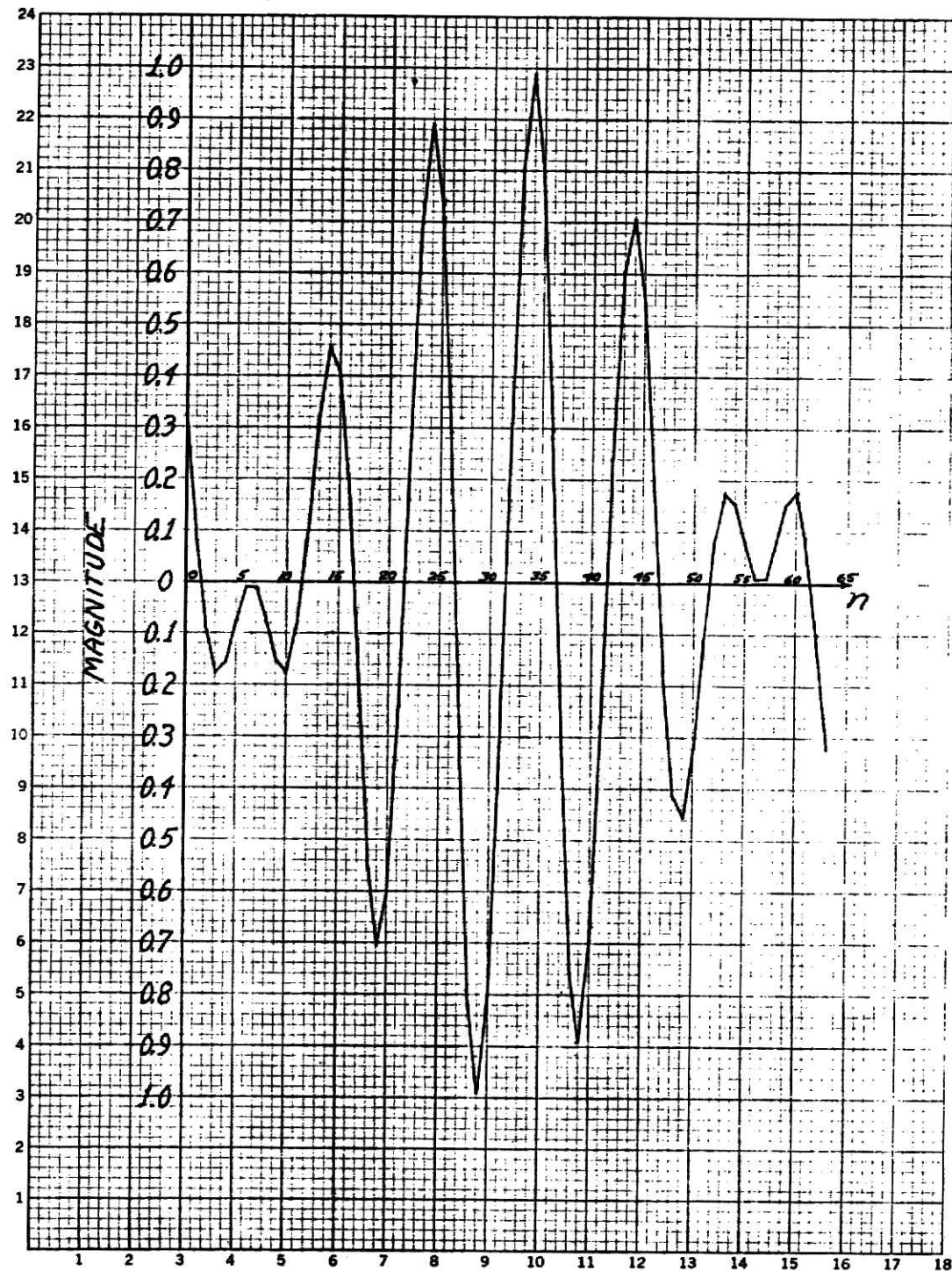
$$\text{time to calculate FFT} \approx \beta 512 \log_2 512.$$

The time for the other calculations involved in the CZT algorithm has been neglected. β is a constant that depends on the FFT program.

It should be apparent that the smaller the frequency band of interest as a fraction of the necessary sampling frequency, the greater is the advantage of the CZT in providing high resolution data within that narrow band. This advantage results from the CZT's flexibility which allows us to evaluate M equally spaced points within a frequency band of arbitrary width without having to evaluate the z-transform outside the band as the FFT requires.

Figure (3-11b) shows a 5 Hz. resolution CZT of the filter over the range $840 \leq f \leq 1160$. In this case, a single 2048 point FFT would have yielded approximately the same 5 Hz. resolution as did the 64 point CZT which used three 128 point FFT's. Assuming that the bulk of the CZT computing time is spent in the FFT subroutine, the 2048 point FFT would have taken approximately 8.5 times as long to calculate as the 64 point CZT.

The size of the comparable FFT's could have been reduced somewhat if the sampling frequency could have been reduced. However, this is usually not possible. Also it would not be strictly correct to compare an FFT and a CZT unless they both use exactly the same data sequence (except for added



5 Squares to the Centimeter

Fig. 3-9. A truncated filter impulse response, a plot of Eq. (3-3).

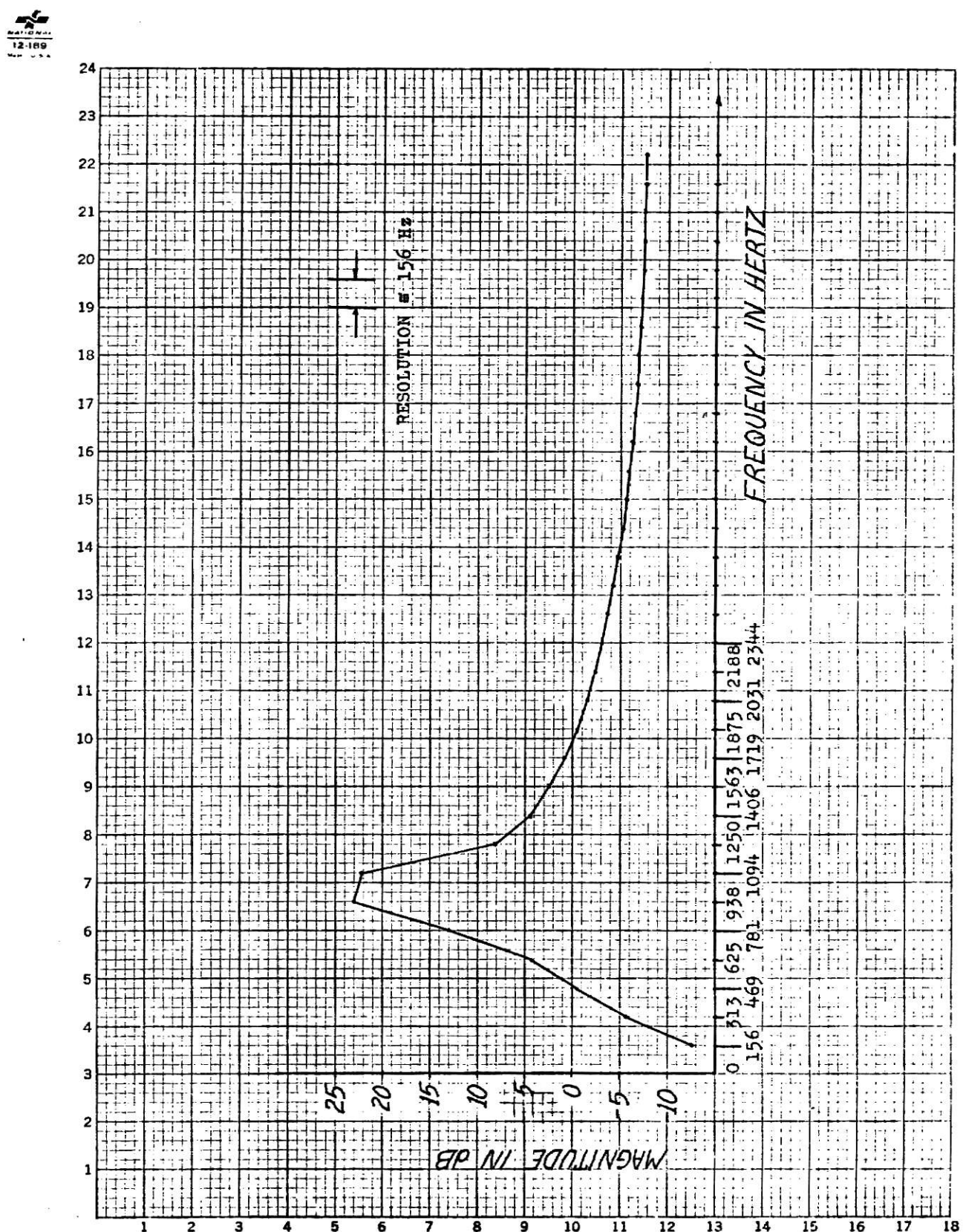


Fig. 3-10. FFT computed frequency response of filter.

12-169

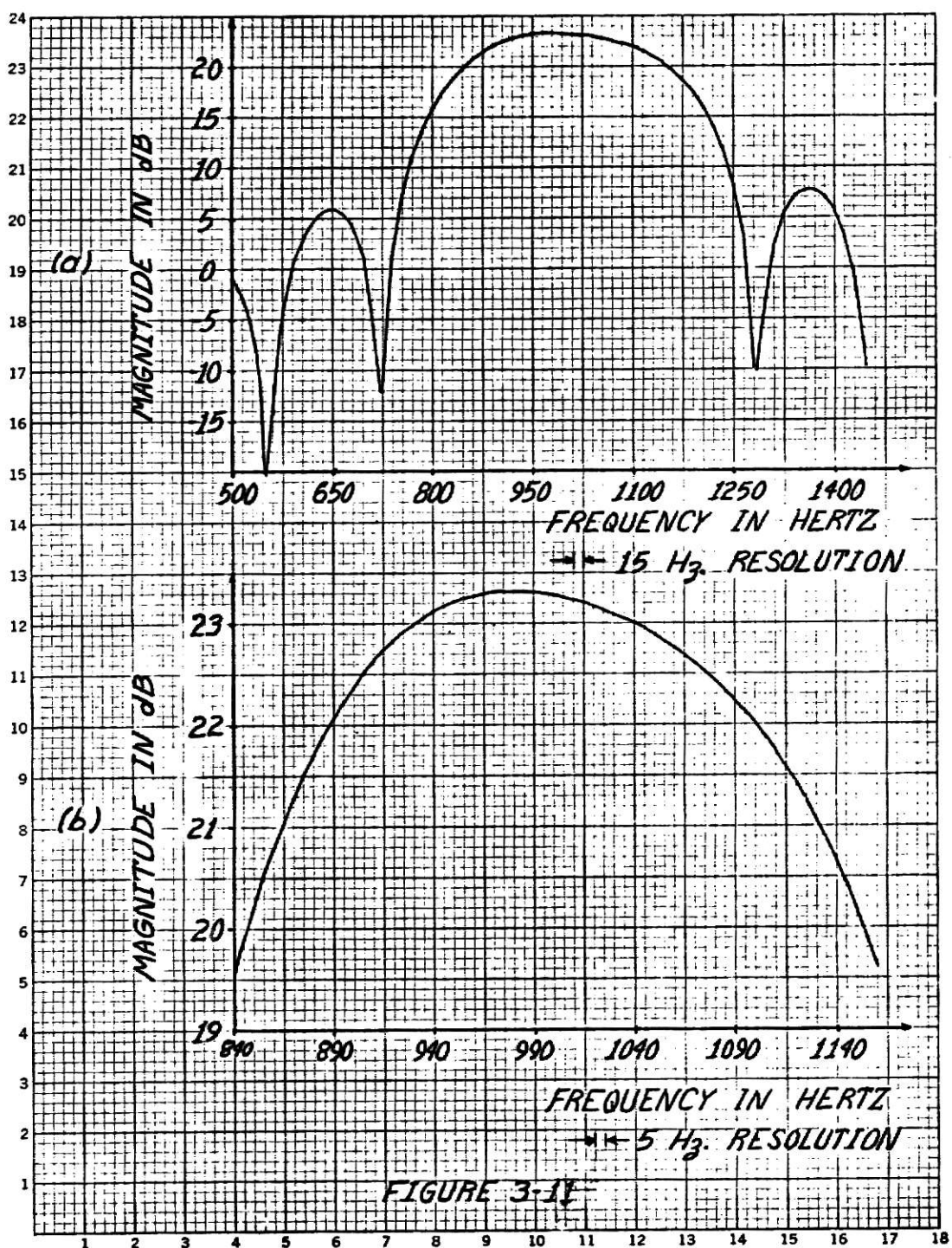


Fig. 3-11. Two CZT computed frequency response plots of filter.

zeroes in the FFT case). The reason for this is that two sample sequences having a different number of samples and/or different sampling rates would really represent two different functions. In other words, their respective finite z-transforms would be two different approximations to the exact z-transform of an infinite number of samples.

Thus the flexibilities of the CZT's frequency spacing and initial frequency allow one to evaluate narrow band spectra much more efficiently than the FFT does.

3.3 Limitations

The principal limitation of the CZT is that we cannot, in practice, evaluate the CZT equally well along all contours. For a given contour off the unit circle, increasing either M or N beyond some value will cause a program interrupt. Likewise, for a given M and N, increasing the $\Delta\sigma$ (ie., $(1/T)\ln W_0$) of the s-plane contour beyond some point will also cause a program interrupt. This results from the fact that the CZT must compute the following numbers:

$$A^{-n} W^{n^2/2} \quad n = 0, 1, \dots, N-1$$

$$W^{-(n^2/2)} \quad n = \begin{cases} 0, 1, \dots, N-1, & N > M \\ 0, 1, \dots, M-1, & M \geq N \end{cases}$$

$$W^{n^2/2} \quad n = 0, 1, \dots, M-1. \quad W = W_0 e^{j2\pi\phi_0}$$

Unless $W_0 = 1$, there will be some M or N for which one of the numbers above will become large or small enough to exceed the floating point capacity of the computer. Hence the program will terminate on an exponent overflow (or underflow) interrupt. If this problem occurs, a trial and error approach is probably the only means available of eliminating the problem. Any of the following measures would need to be taken (individually or in combination):

- (1) change W_0 to be more nearly equal to 1, ie. make the s-plane contour more nearly vertical
- (2) reduce M
- (3) reduce N

If it were undesirable to change W_0 or N, the contour could be divided into several pieces. Each piece could then be evaluated by the CZT separately. Thus we would have reduced M for each individual CZT computation yet still evaluated the entire contour.

In practice it was found that if any of the numbers $(A^{-n}W^{n^2/2}, W^{\pm n^2/2})$ had base 10 exponents whose magnitudes exceeded approximately 35 to 40, an overflow interrupt resulted. The magnitude of a floating point number on the IBM 360/50 is limited to approximately $10^{\pm 75}$ (single or double precision).

Another limitation of the CZT again concerns the numbers $A^{-n}W^{n^2/2}$ and $W^{\pm n^2}$. The CZT program which is listed in this report computes the numbers $A^{-n}W^{n^2/2}$ and $W^{\pm n^2}$ using recursive routines. This method was chosen in order to save computation time. Double precision numbers were used in the program to minimize the round-off and truncation errors. These errors should be unimportant for any L of moderate size.

CHAPTER IV

SUMMARY AND RECOMMENDATIONS

4.1 Summary and Conclusions

In this paper it was shown that the chirp z-transform (CZT) is an algorithm for evaluating the z-transform of a sequence of N numbers at M equi-angularly spaced points on a fairly general contour. Furthermore, M and N are completely arbitrary. The contour can be chosen to be any arbitrary straight line segment in the s-plane. The output point spacing along the contour is also arbitrary as long as it is uniform.

The key to economically computing the CZT lies in expressing the CZT defining equation as a discrete convolution. One can then utilize the capability of the FFT to perform the convolution and thus be able to efficiently evaluate the CZT.

One application of the CZT that was demonstrated was that of sharpening spectral resonances in order to more accurately detect and determine the frequency of the poles producing the resonant peaks. This application assumes that we have some a priori knowledge of where the poles are located. The impulse response of a simple 3-pole system was simulated on a digital computer and its FFT and an appropriate CZT were computed. The CZT was seen to have an advantage over the FFT in this application due to the CZT's capability of evaluating the z-transform off the unit circle.

The second application of the CZT that was demonstrated was that of obtaining high resolution spectral data over a frequency band that was narrow compared to the sampling frequency. In this case a simple digital filter impulse response was simulated on a digital computer and its spectrum evaluated using both the FFT and the CZT. For this application the CZT was

evaluated on the unit circle ($j\omega$ -axis of s-plane). For the purpose of evaluating the filter transfer function in the passband, the CZT was demonstrated to be able to produce high resolution data much more economically relative to the FFT. This advantage results from the CZT's arbitrary output point spacing feature.

Thus the CZT is seen to be the rival of the FFT for some spectral analysis problems. The CZT's capability of evaluating the z-transform off the unit circle ($j\omega$ -axis in s-plane) and its flexible output spacing make it a more valuable tool than the FFT for some applications.

4.2 Recommendations for Further Investigation

One specific problem that arises in anti-submarine warfare might be effectively handled by the CZT*. The problem is that of detecting the random occurrence of a noisy transient sinusoid of known frequency and duration. The capabilities of the CZT to evaluate the z-transform off the unit circle and over a small frequency band might prove valuable. However, this problem is more difficult than the sharpening of spectral resonances since the CZT must deal with very noisy data. The effects that noise has on the z-transform computed off the unit circle would need to be determined. Also this problem requires real time processing of the data. This would require the CZT to be computed repeatedly on a continuous stream of data. Its capabilities in this respect would need to be investigated.

*Suggested by Dr. D.R. Hummels, Dept. of Electrical Engineering,
Kansas State University, Manhattan, Kansas 66502

SELECTED REFERENCES

1. L. R. Rabiner, R. W. Schafer, and C. M. Rader, "The Chirp Z-Transform Algorithm and its Application," *The Bell System Technical Journal*, Vol. 48, No. 5, May-June 1969, pp.1249-1292.
2. D. K. Cheng, *Analysis of Linear Systems*, Addison-Wesley, 1959.
3. N. Ahmed, *An Introduction to Signal Representation and Classification*, (Manuscript to be published by Springer-Verlag).
4. J. W. Cooley and J. W. Tukey, "An Algorithm for the Machine Calculation of Complex Fourier Series," *Mathematics of Computation*, Vol. 19, pp.297-301, 1965.
5. L. I. Bluestein, "A Linear Filtering Approach to the Computation of the Discrete Fourier Transform," *Nerem Record*, pp.218-219, 1968.
6. J. L. Flanagan, *Speech Analysis Synthesis and Perception*, Springer-Verlag, 1965.
7. M. R. Schroeder, "Vocoders: Analysis and Synthesis of Speech," *Proc. IEEE*, Vol. 54, May 1966, pp.720-734.
8. J. L. Flanagan, C. H. Coker, L. R. Rabiner, R. W. Schafer and N. Umeda, "Synthetic Voices for Computers," *IEEE Spectrum*, Vol. 7, No. 10, October 1970, pp.22-45.

APPENDIX

```

S JCB      COMPLEX*16 XDC(128), Y16(128), CMPLX
1       COMPLEX*8 YR(128), XFAVE(128), CNPLX
2       REAL*8 SPEC(128)
3       REAL*8 RMAG,PSPEC(128),DLOG10,CDABS,
4       DATA NMREAD,'PQINT5.6/',
5       PI*3.141593
6
7       ARG1R=C*0.32*PI
8       ARG1I=0.2*PI
9       ARG2R=0.02*PI
10      ARG2I=C*7.2*PI
11      AJZR=0.016*PI
12      ARG3I=0.4*PI
13      DO 100 J=1,64
14      TIME2 =J-1
15      XSAVE(J)=EXP(1.0*TIME*ARG1I)*SIN(1.0*TIME*ANG1I) + EXP(1.0*TIME*ANG2I)*SIN(1.0*TIME*ANG3I)
16      1E+0*ANG2I + EXP(1.0*TIME*ARG3R)*SIN(1.0*TIME*ANG3I)
17      VDC(J)=XSAVE(J)
18
19      CONTINUE
20      END
21      SUBROUTINE FFT(NU,M,Y,I1,I2)
22      C
23      C      - FAST FOURIER TRANSFORM
24      C
25      C THIS PROGRAM COMPUTES THE DFT OF A SEQUENCE X
26      C THE OUTPUT VECTOR IS Y
27      C I1=0 IMPLIES THAT THE PROGRAM COMPUTES THE DFT
28      C I1=1 IMPLIES THAT THE PROGRAM COMPUTES THE IDFT
29      C THE NUMBER OF INPUT AND OUTPUT POINTS,NUM, MUST BE A POWER OF 2
30      C
31      C THE DEFINITION OF THE DFT USED IN THIS PROGRAM HAS THE 1/N FACTOR
32      C ASSOCIATED WITH THE INVERSE TRANSFORM
33
34      IMPLICIT REAL*8(A-H,O-Z)
35      DIMENSION TUP1(110)
36      REAL*4 TUP14
37      COMPLEX*16 X(128),Y(128),ALPHA(128),ALPHI,DCMPLX,DCUR,JG
38      TUP14=.14159265358979312
39      TUP1=COMPLEX(TUP14)
40      I=2
41      I1=1
42      D1=5
43      I=2,11
44      I=11,10
45      I=10,9
46      I=9,8
47      I=8,7
48      I=7,6
49      I=6,5
50      I=5,4
51      I=4,3
52      I=3,2
53      I=2,1
54      I=1,0
55      I=0,1
56      IF (I1.GT.1) GO TO 49
57      IF (I1.EQ.1) ALPHI=DCMPLX(DCOS((TUP1/NUM)*(DCSIN(TUP1/NUM))),-(DCSIN(TUP1/NUM),(DCSIN(TUP1/NUM)))
58      IF (I1.EQ.0) ALPHI=(DCMPLX(DCOS((TUP1/NUM),-(DCSIN(TUP1/NUM),(DCSIN(TUP1/NUM))))))
59      I=1
60      I=1,IPUM,2,IPUM-1
61      IPUM=IPUM-1
62

```

```

41      DO 20 I=1,IP
42      ALPHA(I)=ALPH(I)
43      ALPHA(1)=ALPH(1)-CONJF(ALPHA(1))
44      ALPHA((IBA+1))=ALPH((IBA+1))
45      ALPHA((IBA+NUM-1))=DCONJ(ALPHA((IBA+1)))
46      ALPHA(NUM)=DCMPLX(.0000000, .0000000)
47      ALPHA((IBA))=DCMPLX(-.0000000, .0000000)
48      21 U) 50 M=1,ITER
49      NUM=IPPOWER(B,M)
50      MUM2=IPPOWER(ITER+1-M)
51      MH=IT//2+2-M
52      U=49 IP=1,UMP
53      IP=(IP+1)*IPOWER(MB)
54      IBC=MPI-1
55      IP=0
56      UJ 4 I=MH, ITER
57      IF (IBCD0.0) GO TO 17
58      IU=IPPOWER(ITER-I+1)
59      IF (IU>IBA-LT+1) GO TO 4
60      IBC=IBC-IBA
61      IP=IP+IPPOWER(I-1)
62      C04T14UF
63      17 IP=IP+.001 IP=NUM
64      00 48 MP2=1,NUM2
65      IBA=IB*MP2
66      MUM2=MUM2+IBA
67      ALPHA(IP*X(MNUM2))
68      Y(IBA)=X(IBA)+ALPH
69      Y(M*UM2)=X(IBA)-ALPH
70      48 C04T14UF
71      49 CONTINUE
72      09 7 I=1,NUM
73      7 A(I)=Y(I)
74      50 CONTINUE
75      RUM=1.00000000
76      ITII=.5E-11 RUMM=1.0000000/NUM
77      DO 11 I=1,NUM
78      IB=I-1
79      IP=1
80      DO 9 ITI=1,ITER
81      ITI=.5E-11 RUMM=1.00000000 GO TO 11
82      ICA=IPCMPOWER(ITII+1),
83      ITI=IB-LT+1 GO TO 9
84      IA=IB-IBA
85      IP=IP+IPPOWER(ITII),
86      C04T14UF
87      11 Y(IP)=X(I)*RUM
88      599 RETURN
89      END
90      C
91      C
92      C
93      C
94      C
95      C
96      C
97      C
98      C
99      C
100     C
101     C
102     C
103     C
104     C
105     C
106     C
107     C
108     C
109     C
110     C
111     C
112     C
113     C
114     C
115     C
116     C
117     C
118     C
119     C
120     C
121     C
122     C
123     C
124     C
125     C
126     C
127     C
128     C
129     C
130     C
131     C
132     C
133     C
134     C
135     C
136     C
137     C
138     C
139     C
140     C
141     C
142     C
143     C
144     C
145     C
146     C
147     C
148     C
149     C
150     C
151     C
152     C
153     C
154     C
155     C
156     C
157     C
158     C
159     C
160     C
161     C
162     C
163     C
164     C
165     C
166     C
167     C
168     C
169     C
170     C
171     C
172     C
173     C
174     C
175     C
176     C
177     C
178     C
179     C
180     C
181     C
182     C
183     C
184     C
185     C
186     C
187     C
188     C
189     C
190     C
191     C
192     C
193     C
194     C
195     C
196     C
197     C
198     C
199     C
200     C
201     C
202     C
203     C
204     C
205     C
206     C
207     C
208     C
209     C
210     C
211     C
212     C
213     C
214     C
215     C
216     C
217     C
218     C
219     C
220     C
221     C
222     C
223     C
224     C
225     C
226     C
227     C
228     C
229     C
230     C
231     C
232     C
233     C
234     C
235     C
236     C
237     C
238     C
239     C
240     C
241     C
242     C
243     C
244     C
245     C
246     C
247     C
248     C
249     C
250     C
251     C
252     C
253     C
254     C
255     C
256     C
257     C
258     C
259     C
260     C
261     C
262     C
263     C
264     C
265     C
266     C
267     C
268     C
269     C
270     C
271     C
272     C
273     C
274     C
275     C
276     C
277     C
278     C
279     C
280     C
281     C
282     C
283     C
284     C
285     C
286     C
287     C
288     C
289     C
290     C
291     C
292     C
293     C
294     C
295     C
296     C
297     C
298     C
299     C
300     C
301     C
302     C
303     C
304     C
305     C
306     C
307     C
308     C
309     C
310     C
311     C
312     C
313     C
314     C
315     C
316     C
317     C
318     C
319     C
320     C
321     C
322     C
323     C
324     C
325     C
326     C
327     C
328     C
329     C
330     C
331     C
332     C
333     C
334     C
335     C
336     C
337     C
338     C
339     C
340     C
341     C
342     C
343     C
344     C
345     C
346     C
347     C
348     C
349     C
350     C
351     C
352     C
353     C
354     C
355     C
356     C
357     C
358     C
359     C
360     C
361     C
362     C
363     C
364     C
365     C
366     C
367     C
368     C
369     C
370     C
371     C
372     C
373     C
374     C
375     C
376     C
377     C
378     C
379     C
380     C
381     C
382     C
383     C
384     C
385     C
386     C
387     C
388     C
389     C
390     C
391     C
392     C
393     C
394     C
395     C
396     C
397     C
398     C
399     C
400     C
401     C
402     C
403     C
404     C
405     C
406     C
407     C
408     C
409     C
410     C
411     C
412     C
413     C
414     C
415     C
416     C
417     C
418     C
419     C
420     C
421     C
422     C
423     C
424     C
425     C
426     C
427     C
428     C
429     C
430     C
431     C
432     C
433     C
434     C
435     C
436     C
437     C
438     C
439     C
440     C
441     C
442     C
443     C
444     C
445     C
446     C
447     C
448     C
449     C
450     C
451     C
452     C
453     C
454     C
455     C
456     C
457     C
458     C
459     C
460     C
461     C
462     C
463     C
464     C
465     C
466     C
467     C
468     C
469     C
470     C
471     C
472     C
473     C
474     C
475     C
476     C
477     C
478     C
479     C
480     C
481     C
482     C
483     C
484     C
485     C
486     C
487     C
488     C
489     C
490     C
491     C
492     C
493     C
494     C
495     C
496     C
497     C
498     C
499     C
500     C
501     C
502     C
503     C
504     C
505     C
506     C
507     C
508     C
509     C
510     C
511     C
512     C
513     C
514     C
515     C
516     C
517     C
518     C
519     C
520     C
521     C
522     C
523     C
524     C
525     C
526     C
527     C
528     C
529     C
530     C
531     C
532     C
533     C
534     C
535     C
536     C
537     C
538     C
539     C
540     C
541     C
542     C
543     C
544     C
545     C
546     C
547     C
548     C
549     C
550     C
551     C
552     C
553     C
554     C
555     C
556     C
557     C
558     C
559     C
560     C
561     C
562     C
563     C
564     C
565     C
566     C
567     C
568     C
569     C
570     C
571     C
572     C
573     C
574     C
575     C
576     C
577     C
578     C
579     C
580     C
581     C
582     C
583     C
584     C
585     C
586     C
587     C
588     C
589     C
590     C
591     C
592     C
593     C
594     C
595     C
596     C
597     C
598     C
599     C
600     C
601     C
602     C
603     C
604     C
605     C
606     C
607     C
608     C
609     C
610     C
611     C
612     C
613     C
614     C
615     C
616     C
617     C
618     C
619     C
620     C
621     C
622     C
623     C
624     C
625     C
626     C
627     C
628     C
629     C
630     C
631     C
632     C
633     C
634     C
635     C
636     C
637     C
638     C
639     C
640     C
641     C
642     C
643     C
644     C
645     C
646     C
647     C
648     C
649     C
650     C
651     C
652     C
653     C
654     C
655     C
656     C
657     C
658     C
659     C
660     C
661     C
662     C
663     C
664     C
665     C
666     C
667     C
668     C
669     C
670     C
671     C
672     C
673     C
674     C
675     C
676     C
677     C
678     C
679     C
680     C
681     C
682     C
683     C
684     C
685     C
686     C
687     C
688     C
689     C
690     C
691     C
692     C
693     C
694     C
695     C
696     C
697     C
698     C
699     C
700     C
701     C
702     C
703     C
704     C
705     C
706     C
707     C
708     C
709     C
710     C
711     C
712     C
713     C
714     C
715     C
716     C
717     C
718     C
719     C
720     C
721     C
722     C
723     C
724     C
725     C
726     C
727     C
728     C
729     C
730     C
731     C
732     C
733     C
734     C
735     C
736     C
737     C
738     C
739     C
740     C
741     C
742     C
743     C
744     C
745     C
746     C
747     C
748     C
749     C
750     C
751     C
752     C
753     C
754     C
755     C
756     C
757     C
758     C
759     C
760     C
761     C
762     C
763     C
764     C
765     C
766     C
767     C
768     C
769     C
770     C
771     C
772     C
773     C
774     C
775     C
776     C
777     C
778     C
779     C
780     C
781     C
782     C
783     C
784     C
785     C
786     C
787     C
788     C
789     C
790     C
791     C
792     C
793     C
794     C
795     C
796     C
797     C
798     C
799     C
800     C
801     C
802     C
803     C
804     C
805     C
806     C
807     C
808     C
809     C
810     C
811     C
812     C
813     C
814     C
815     C
816     C
817     C
818     C
819     C
820     C
821     C
822     C
823     C
824     C
825     C
826     C
827     C
828     C
829     C
830     C
831     C
832     C
833     C
834     C
835     C
836     C
837     C
838     C
839     C
840     C
841     C
842     C
843     C
844     C
845     C
846     C
847     C
848     C
849     C
850     C
851     C
852     C
853     C
854     C
855     C
856     C
857     C
858     C
859     C
860     C
861     C
862     C
863     C
864     C
865     C
866     C
867     C
868     C
869     C
870     C
871     C
872     C
873     C
874     C
875     C
876     C
877     C
878     C
879     C
880     C
881     C
882     C
883     C
884     C
885     C
886     C
887     C
888     C
889     C
890     C
891     C
892     C
893     C
894     C
895     C
896     C
897     C
898     C
899     C
900     C
901     C
902     C
903     C
904     C
905     C
906     C
907     C
908     C
909     C
910     C
911     C
912     C
913     C
914     C
915     C
916     C
917     C
918     C
919     C
920     C
921     C
922     C
923     C
924     C
925     C
926     C
927     C
928     C
929     C
930     C
931     C
932     C
933     C
934     C
935     C
936     C
937     C
938     C
939     C
940     C
941     C
942     C
943     C
944     C
945     C
946     C
947     C
948     C
949     C
950     C
951     C
952     C
953     C
954     C
955     C
956     C
957     C
958     C
959     C
960     C
961     C
962     C
963     C
964     C
965     C
966     C
967     C
968     C
969     C
970     C
971     C
972     C
973     C
974     C
975     C
976     C
977     C
978     C
979     C
980     C
981     C
982     C
983     C
984     C
985     C
986     C
987     C
988     C
989     C
990     C
991     C
992     C
993     C
994     C
995     C
996     C
997     C
998     C
999     C
1000    C
1001    C
1002    C
1003    C
1004    C
1005    C
1006    C
1007    C
1008    C
1009    C
1010    C
1011    C
1012    C
1013    C
1014    C
1015    C
1016    C
1017    C
1018    C
1019    C
1020    C
1021    C
1022    C
1023    C
1024    C
1025    C
1026    C
1027    C
1028    C
1029    C
1030    C
1031    C
1032    C
1033    C
1034    C
1035    C
1036    C
1037    C
1038    C
1039    C
1040    C
1041    C
1042    C
1043    C
1044    C
1045    C
1046    C
1047    C
1048    C
1049    C
1050    C
1051    C
1052    C
1053    C
1054    C
1055    C
1056    C
1057    C
1058    C
1059    C
1060    C
1061    C
1062    C
1063    C
1064    C
1065    C
1066    C
1067    C
1068    C
1069    C
1070    C
1071    C
1072    C
1073    C
1074    C
1075    C
1076    C
1077    C
1078    C
1079    C
1080    C
1081    C
1082    C
1083    C
1084    C
1085    C
1086    C
1087    C
1088    C
1089    C
1090    C
1091    C
1092    C
1093    C
1094    C
1095    C
1096    C
1097    C
1098    C
1099    C
1100    C
1101    C
1102    C
1103    C
1104    C
1105    C
1106    C
1107    C
1108    C
1109    C
1110    C
1111    C
1112    C
1113    C
1114    C
1115    C
1116    C
1117    C
1118    C
1119    C
1120    C
1121    C
1122    C
1123    C
1124    C
1125    C
1126    C
1127    C
1128    C
1129    C
1130    C
1131    C
1132    C
1133    C
1134    C
1135    C
1136    C
1137    C
1138    C
1139    C
1140    C
1141    C
1142    C
1143    C
1144    C
1145    C
1146    C
1147    C
1148    C
1149    C
1150    C
1151    C
1152    C
1153    C
1154    C
1155    C
1156    C
1157    C
1158    C
1159    C
1160    C
1161    C
1162    C
1163    C
1164    C
1165    C
1166    C
1167    C
1168    C
1169    C
1170    C
1171    C
1172    C
1173    C
1174    C
1175    C
1176    C
1177    C
1178    C
1179    C
1180    C
1181    C
1182    C
1183    C
1184    C
1185    C
1186    C
1187    C
1188    C
1189    C
1190    C
1191    C
1192    C
1193    C
1194    C
1195    C
1196    C
1197    C
1198    C
1199    C
1200    C
1201    C
1202    C
1203    C
1204    C
1205    C
1206    C
1207    C
1208    C
1209    C
1210    C
1211    C
1212    C
1213    C
1214    C
1215    C
1216    C
1217    C
1218    C
1219    C
1220    C
1221    C
1222    C
1223    C
1224    C
1225    C
1226    C
1227    C
1228    C
1229    C
1230    C
1231    C
1232    C
1233    C
1234    C
1235    C
1236    C
1237    C
1238    C
1239    C
1240    C
1241    C
1242    C
1243    C
1244    C
1245    C
1246    C
1247    C
1248    C
1249    C
1250    C
1251    C
1252    C
1253    C
1254    C
1255    C
1256    C
1257    C
1258    C
1259    C
1260    C
1261    C
1262    C
1263    C
1264    C
1265    C
1266    C
1267    C
1268    C
1269    C
1270    C
1271    C
1272    C
1273    C
1274    C
1275    C
1276    C
1277    C
1278    C
1279    C
1280    C
1281    C
1282    C
1283    C
1284    C
1285    C
1286    C
1287    C
1288    C
1289    C
1290    C
1291    C
1292    C
1293    C
1294    C
1295    C
1296    C
1297    C
1298    C
1299    C
1300    C
1301    C
1302    C
1303    C
1304    C
1305    C
1306    C
1307    C
1308    C
1309    C
1310    C
1311    C
1312    C
1313    C
1314    C
1315    C
1316    C
1317    C
1318    C
1319    C
1320    C
1321    C
1322    C
1323    C
1324    C
1325    C
1326    C
1327    C
1328    C
1329    C
1330    C
1331    C
1332    C
1333    C
1334    C
1335    C
1336    C
1337    C
1338    C
1339    C
1340    C
1341    C
1342    C
1343    C
1344    C
1345    C
1346    C
1347    C
1348    C
1349    C
1350    C
1351    C
1352    C
1353    C
1354    C
1355    C
1356    C
1357    C
1358    C
1359    C
1360    C
1361    C
1362    C
1363    C
1364    C
1365    C
1366    C
1367    C
1368    C
1369    C
1370    C
1371    C
1372    C
1373    C
1374    C
1375    C
1376    C
1377    C
1378    C
1379    C
1380    C
1381    C
1382    C
1383    C
1384    C
1385    C
1386    C
1387    C
1388    C
1389    C
1390    C
1391    C
1392    C
1393    C
1394    C
1395    C
1396    C
1397    C
1398    C
1399    C
1400    C
1401    C
1402    C
1403    C
1404    C
1405    C
1406    C
1407    C
1408    C
1409    C
1410    C
1411    C
1412    C
1413    C
1414    C
1415    C
1416    C
1417    C
1418    C
1419    C
1420    C
1421    C
1422    C
1423    C
1424    C
1425    C
1426    C
1427    C
1428    C
1429    C
1430    C
1431    C
1432    C
1433    C
1434    C
1435    C
1436    C
1437    C
1438    C
1439    C
1440    C
1441    C
1442    C
1443    C
1444    C
1445    C
1446    C
1447    C
1448    C
1449    C
1450    C
1451    C
1452    C
1453    C
1454    C
1455    C
1456    C
1457    C
1458    C
1459    C
1460    C
1461    C
1462    C
1463    C
1464    C
1465    C
1466    C
1467    C
1468    C
1469    C
1470    C
1471    C
1472    C
1473    C
1474    C
1475    C
1476    C
1477    C
1478    C
1479    C
1480    C
1481    C
1482    C
1483    C
1484    C
1485    C
1486    C
1487    C
1488    C
1489    C
1490    C
1491    C
1492    C
1493    C
1494    C
1495    C
1496    C
1497    C
1498    C
1499    C
1500    C
1501    C
1502    C
1503    C
1504    C
1505    C
1506    C
1507    C
1508    C
1509    C
1510    C
1511    C
1512    C
1513    C
1514    C
1515    C
1516    C
1517    C
1518    C
1519    C
1520    C
1521    C
1522    C
1523    C
1524    C
1525    C
1526    C
1527    C
1528    C
1529    C
1530    C
1531    C
1532    C
1533    C
1534    C
1535    C
1536    C
1537    C
1538    C
1539    C
1540    C
1541    C
1542    C
1543    C
1544    C
1545    C
1546    C
1547    C
1548    C
1549    C
1550    C
1551    C
1552    C
1553    C
1554    C
1555    C
1556    C
1557    C
1558    C
1559    C
1560    C
1561    C
1562    C
1563    C
1564    C
1565    C
1566    C
1567    C
1568    C
1569    C
1570    C
1571    C
1572    C
1573    C
1574    C
1575    C
1576    C
1577    C
1578    C
1579    C
1580    C
1581    C
1582    C
1583    C
1584    C
1585    C
1586    C
1587    C
1588    C
1589    C
1590    C
1591    C
1592    C
1593    C
1594    C
1595    C
1596    C
1597    C
1598    C
1599    C
1600    C
1601    C
1602    C
1603    C
1604    C
1605    C
1606    C
1607    C
1608    C
1609    C
1610    C
1611    C
1612    C
1613    C
1614    C
1615    C
1616    C
1617    C
1618    C
1619    C
1620    C
1621    C
1622    C
1623    C
1624    C
1625    C
1626    C
1627    C
1628    C
1629    C
1630    C
1631    C
1632    C
1633    C
1634    C
1635    C
1636    C
1637    C
1638    C
1639    C
1640    C
1641    C
1642    C
1643    C
1644    C
1645    C
1646    C
1647    C
1648    C
1649    C
1650    C
1651    C
1652    C
1653    C
1654    C
1655    C
1656    C
1657    C
1658    C
1659    C
1660    C
1661    C
1662    C
1663    C
1664    C
1665    C
1666    C
1667    C
1668    C
1669    C
1670    C
1671    C
1672    C
1673    C
1674    C
1675    C
1676    C
1677    C
1678    C
1679    C
1680    C
1681    C
1682    C
1683    C
1684    C
1685    C
1686    C
1687    C
1688    C
1689    C
1690    C
1691    C
1692    C
1693    C
1694    C
1695    C
1696    C
1697    C
1698    C
1699    C
1700    C
1701    C
1702    C
1703    C
1704    C
1705    C
1706    C
1707    C
1708    C
1709    C
1710    C
1711    C
1712    C
1713    C
1714    C
1715    C
1716    C
1717    C
1718    C
1719    C
1720    C
1721    C
1722    C
1723    C
1724    C
1725    C
1726    C
1727    C
1728    C
1729    C
1730    C
1731    C
1732    C
1733    C
1734    C
1735    C
1736    C
1737    C
1738    C
173
```

C THE FOLLOWING PARAMETERS MUST BE COMMUNICATED TO THE PROGRAM
 C
 C NN IS THE NUMBER OF DATA POINTS (ARBITRARY)
 C M IS THE DESIRED NUMBER OF EVALUATION POINTS (ARBITRARY)
 C L MUST BE A NUMBER WHICH IS AN INTEGER POWER OF TWO
 C AND IS $\geq M \cdot N - 1$
 C THE FOLLOWING ALSO MUST ALL BE GIVEN IN DOUBLE PRECISION
 C RAMP IS THE MAGNITUDE OF A
 C RWAG IS THE MAGNITUDE OF A
 C RWPH IS THE FACTOR IN THE INITIAL ANGLE THETA (THETA=2*pi*RAPH)
 C DIMENSION QSIGMA(128),ROMEGA(128)
 C EQUIVALENCE W(1),X(1) * W(1),GK(1),XK(1)
 C DATA NRAD,NPRINT/5,6/
 C N=64
 C M=65
 C L=128
 C K1=4
 C K1=4
 C R2P=6.283186
 C P2PI=UNL(4*2pi)
 C RAPMAG=0.00000000
 C RAPH=0.00000000
 C RMPhi=0.5000000000/FNN
 C RMAG=DFXP(-R2P1*RbPhi/40.)
 C T=J-COD20000000
 C RPI=M+1
 C RPI=M+1
 C ARKAMAG=DCMPLX(DCOS(R2P1*RAPH)*DSIN(R2P1*RAPH))
 C W=RMAG*DCMPLX(DCOS(R2P1*RAPH),USIN(R2P1*RAPH))
 C
 C PRINT 44 ECHO CHECK OF THE DATA
 C
 C 114 WRITE(*,*)'POINT 103'
 C 103 FORMAT (1HO,*ECHO CHECK OF INPUT VALUES //)
 C 115 WRITE(*,*)'POINT 101', (X(I), I=1,NN)
 C 116 1.001 1.001 0.00000000 0.00000000
 C 117 0.2F15.51 0.0F000000 0.0F000000
 C 118 WLOG=CHLOG(W)
 C 119 D1=C2*AP10*50000000+WLOG
 C 120 D1=D1/A
 C 121
 C BEGIN A RECURSIVE ROUTINE TO FORM AN L POINT SEQUENCE FROM THE
 C INPUT DATA
 C
 C THE FIRST NN POINTS OF THE SEQUENCE ARE FORMED BY APPROPRIATELY WEIGHTING
 C THE INPUT DATA POINTS
 C
 C 122 00 100 M=2,41
 C 123 C1=CHD1
 C 124 D1=D1/A

```

125      K(V)=CNP1*K(N)
126      CN=CNP1
127      ICO
128      C   THE REMAINING L-NN POINTS ARE SET EQUAL TO ZERO
129      DO 105 I= NIP1,L
130      105 X(I)=10.0000000 + 0.0000000I
131      C   COMPUTE THE L POINT DFT OF THE SEQUENCE JUST FORMED. CALL THE DFT
132      C   SEQUENCE Y.
133      C   BEGIN A RECURSIVE ROUTINE TO CONSTRUCT THE L POINT SEQUENCE VN
134      C   WHILE AR= TWO PATHS THROUGH THIS ROUTINE DEPENDING ON WHICH
135      C   IS LARGER, M OR NN
136      IF (M>GF*NN) GO TO 750
137      E(1)=11.0000000 + 0.0000000I
138      J=1-1
139      E(1)=E(1)*F
140      F=F/W
141      V(1,J)=E(1)
142      IF (N.LE.M) VN(N)=E(1)
143      230  CONTINUE
144      E(1)=11.0000000 + 0.0000000I
145      F=CEXP(-0.5000000*FLUC)
146      V(1,1)=E(1)
147      DO 260 N=2,M
148      J=1-1
149      E(1)=E(1)*F
150      F=F/W
151      V(1,1)=E(1)
152      IF (N.LE.NV) VN(J)=E(1)
153      260  CONTINUE
154      C   IF LE=MNV-1 THERE ARE NO ARBITRARY TERMS IN VN
155      C   IF L>=M+MN-1 SET ARBITRARY TERMS= 0
156      IF (L>=0 .AND. (M+MN-1)) GO TO 285
157      MK=L-N+1
158      DO 280 N=MPL,MK
159      VN(N)=10.000000 + 0.0000000I
160      285  CONTINUE
161      C   COMPUTE THE L POINT DFT OF THE SEQUENCE VN, CALL THE DFT SUBROUTINE V
162      285 I=0
163      CALL FFT(L,V,N,I)
164      C   MULTIPLY THE TWO DFT SEQUENCES, Y AND VN, POINT BY POINT TO VN.LU THE
165      C   SEQUENCE G

```


0.16436	0.00000
-0.81019	0.00000
-0.32423	0.00000
-0.29571	0.00000
0.26174	0.00000
-0.32367	0.00000
0.84639	0.00000
-0.01294	0.00000
-0.39115	0.00000
-0.09161	0.00000
0.67650	0.00000
-0.92234	0.00000
0.39090	0.00000
-0.26421	0.00000
0.00000	0.00000
-0.02313	0.00000
0.48577	0.00000
-0.34208	0.00000
0.31351	0.00000
0.66002	0.00000
0.02647	0.00000
-0.23629	0.00000
-0.27452	0.00000
0.17242	0.00000
-0.09502	0.00000
-0.02577	0.00000
-0.21833	0.00000
0.23629	0.00000
-0.17242	0.00000
0.07044	0.00000
-0.02672	0.00000
-0.14678	0.00000
0.10649	0.00000
0.31496	0.00000
-0.22892	0.00000
0.07044	0.00000
-0.02672	0.00000
-0.14678	0.00000
0.10649	0.00000
-0.07974	0.00000
0.05870	0.00000
-0.03046	0.00000
0.06341	0.00000
-0.03242	0.00000
-0.00495	0.00000
0.06340	0.00000
-0.12757	0.00000
0.11613	0.00000
-0.08076	0.00000
-0.00556	0.00000
0.07157	0.00000
-0.09446	0.00000
0.09138	0.00000
-0.04499	0.00000
0.00701	0.00000
0.01541	0.00000
-0.02755	0.00000
0.02146	0.00000
-0.02767	0.00000
0.03245	0.00000
-0.01664	0.00000
0.23446	0.00000
-0.00511	0.00000

VALUES OF Z-TRANSFORM OF X(t)		POWER SPECTRUM JF(X(t))		FREQUENCY IN HERTZ	
REAL	IMAGINARY	REAL	IMAGINARY	FR-Q.	FR-Q.
1.8676087833	0.0000001575	3.48796	5.42532	0.0.0.0.0	0.0.0.0.0
1.8664344327	-0.0381659368	3.48506	5.42211	-0.7656	-0.7656
1.9053734457	-0.078216771	3.03720	5.00767	-1.0534	-1.0534
1.9399866257	-0.1240091813	3.77897	5.77373	-2.9496	-2.9496
2.0234443003	-0.1763754630	4.12564	6.15670	-3.91625	-3.91625
2.1079430016	-0.245927676	4.49546	6.52775	-4.1228	-4.1228
2.256891759	-0.3359827750	5.19426	7.45534	-5.81937	-5.81937
2.4142612680	-0.4698653265	6.04943	7.81714	-6.8559	-6.8559
2.6710804819	-0.6772024890	7.58620	8.00256	-7.8450	-7.8450
2.9619938024	-1.08666290	9.80699	9.91535	-8.7196	-8.7196
3.3638034301	-1.626241434	1.3.98736	11.45736	-9.7556	-9.7556
3.6305915685	-2.7969225583	2.1.00397	13.22301	-10.7219	-10.7219
4.066377587	-4.06154220	3.1.89887	15.03775	-11.7375	-11.7375
4.086039273	-5.065621612	3.3.72299	15.27976	-12.6723	-12.6723
4.0936378005	-3.9771264348	20.22096	13.05802	-13.6716	-13.6716
4.1810842959	-2.32642615	4.75046	9.80923	-4.64644	-4.64644
4.781613625	-1.262293690	4.78880	6.80226	-15.5250	-15.5250
5.1362726483	-0.8310982801	2.26289	4.08731	-16.6756	-16.6756
5.10576833104	-0.5130073485	1.81238	1.60626	-7.5781	-7.5781
5.7981266085	-0.418831511	0.81343	-0.89661	-16.5467	-16.5467
6.0610198930	-0.249433630	0.43679	-3.59732	-13.5312	-13.5312
6.042317721	-0.262939771	0.26481	-5.77065	-20.5784	-20.5784
6.324217845	-0.1276644674	0.12143	-9.15684	-620.	-620.
6.1945844845	-0.1962024475	0.07636	-11.17142	-620.	-620.
6.1193126956	-0.0579759760	0.01762	-17.54564	-938.	-938.
6.00010951391	-0.169153618	0.02H64	-15.43430	742.	742.
6.0405672393	-0.0997766531	0.01J17	-27.57129	1.116.	1.116.
6.16835664670	-0.1643566275	0.05538	-12.56933	1.655.	1.655.
6.1758691066	-0.1276644674	0.01214	-9.15684	-620.	-620.
6.3341487259	-0.1749516767	0.014226	-11.17142	-620.	-620.
6.2991555434	-0.0664132519	0.09417	-10.26067	1.172.	1.172.
6.51306558660	-0.1989436971	0.01J07	-15.43430	977.	977.
6.419143874	-0.109726H77	0.18772	-7.26456	1.211.	1.211.
6.728115495	-0.2366940671	0.58621	-2.31944	1.250.	1.250.
6.5434155847	-0.1575004444	0.32011	-4.947099	1.094.	1.094.
6.0548144447	-0.2906581072	1.09614	-8.46907	1.133.	1.133.
6.0668193253	-0.214720949	0.50H77	-10.26067	1.172.	1.172.
6.3967683369	-0.3651566031	2.08425	-15.43430	977.	977.
6.4224172373	-0.157653276	30.10545	-7.26456	1.211.	1.211.
6.213143104	-0.2289052681	4.22126	-1.484.	-31.2710	-31.2710
6.0000919526	-0.4674280897	4.95027	6.94679	-32.4656	-32.4656
1.0541561011	0.3603666562	1.44110	-6.947099	1.326.	1.326.
3.0626634416	-0.6104280563	9.75241	0.39868	1.667.	1.667.
1.3909186923	0.416899050	2.10862	-2.93477	1.406.	1.406.
1.4224172373	-0.157653276	30.10545	3.48969	1.645.	1.645.
2.213143104	-0.2289052681	4.22126	1.484.	-37.1.937	-37.1.937
1.5783394442	-2.007523927	253.14576	2.4.03569	-4.2.7.677	-4.2.7.677
3.0760871153	-2.4296747474	606.27130	27.82662	-29.0.2.0.2	-29.0.2.0.2
1.61717610997	-5.9641577667	9.505174	115.08756	-34.0.9.3.0.2	-34.0.9.3.0.2
1.3909186923	-8.3211824374	14.06727	1.1.49214	-4.6.8.7.0.0	-4.6.8.7.0.0
1.1035394316	-3.7913156682	23.498729	1.1.7944	-4.7.5.3.5.6	-4.7.5.3.5.6
1.1334397648	4.711.15336.	24.03567	1.1.7944	-4.9.5.7.6.4	-4.9.5.7.6.4
3.5992139157	-5.6927053919	46.09104	16.0.3615	-4.9.5.7.6.4	-4.9.5.7.6.4
7.775619335	9.5004057426	315.05174	20.0.1.0.35	-2.9.7.2.2	-2.9.7.2.2
35.597702516	-8.3211824374	1.1.49214	3.2.26032	-4.6.8.7.0.0	-4.6.8.7.0.0
-1.5798137054	-3.4016857754	2794.17664	34.0.44537	-5.2.7.9.7	-5.2.7.9.7
-3.1035394316	-1.7913156682	1113.44538	30.4.6667	-5.2.7.9.7	-5.2.7.9.7
-1.1334397648	-4.711.15336.	21.2.364.4	21.2.364.4	-5.2.7.9.7	-5.2.7.9.7
1.3734397648	-4.954437491	7.2344.567127	25.0.00011	-5.2.7.9.7	-5.2.7.9.7
-1.6.37.17.14.06624	-1.6.37.17.14.06624	7.2344.567127	25.0.00011	-5.2.7.9.7	-5.2.7.9.7

```

6.2539336280      -4.8393937616      62.53139      17.96097      2266.
-14.2163676929     4.9549221825      218.60437      23.39658      2305.
6.8048730229      -2.9102454062      34.77579      17.38568      2544.
-14.3411064219     2.3353482733      202.00652      23.06653      2383.
7.4626851343      -1.5034752102      64.08226      18.06737      2422.
-14.7666923962     0.8387623398      224.70541      23.51613      2461.
9.4723369629      -0.0025611163      89.72517      19.52913      2500.
                                         2152 BYTES, TOTAL AREA AVAILABLE = 4452, BYTES

CORE USAGE: OBJECT CODE= 1456 BYTES, ARRAY AREA= 2152 BYTES, TOTAL AREA AVAILABLE = 4452, BYTES

DIAGNOSTICS: NUMBER OF ERRORS= 0, NUMBER OF WARNINGs= 0, NUMBER OF SE= 0
              DATE= 1/17/75

COMPILE TIME= 6.63 SEC, EXECUTION TIME= 11.70 SEC, WAITIV - VERSION 1 LEVEL 3 MARCH 1971   DATE= 1/17/75

```

ACKNOWLEDGEMENT

The author wishes to express his sincere appreciation to his major professor, Dr. Nasir Ahmed, for his valuable guidance and assistance in the preparation of this report.

A STUDY OF THE CHIRP Z-TRANSFORM
AND ITS APPLICATIONS

by

STEVE ALAN SHILLING

B. S., Kansas State University, 1970

AN ABSTRACT OF A MASTER'S REPORT

submitted in partial fulfillment of the

requirements for the degree

MASTER OF SCIENCE

Department of Electrical Engineering

KANSAS STATE UNIVERSITY
Manhattan, Kansas

1972

ABSTRACT

The Chirp Z-Transform (CZT) is developed. The CZT is a computational algorithm which evaluates the z-transform of N data samples at M points along a fairly general contour. The contour is a straight line segment in the s-plane of arbitrary starting point, length, and orientation. M and N are arbitrary integers. The output spacing is an arbitrary constant.

The algorithm is based upon expressing the z-transform to be evaluated along the prescribed contour as a discrete convolution. The FFT can then be used to compute this convolution efficiently.

Applications of the CZT that are demonstrated include: enhancement of poles in spectral analysis, and high frequency narrow-band frequency analysis.